

## Replies to Anonymous Referee #1

Original comments received and published: 16 December 2019

### GENERAL COMMENTS

This paper outlines the use of cyclone tracking to identify some key points of the climate and weather over the North Atlantic and Western Europe during that Last Glacial Maximum (LGM). The paper identifies changes in the mean state that may be both conducive to dust emission (e.g. increase in wind speeds) and also those which may hinder it (e.g. more storm activity and associated precipitation). The key point in the authors' analysis is the cyclone tracking and compositing, which provides important information on how the mean climate state is felt at the surface through the extratropical cyclones (in this case, the 30 most extreme). It is very clear from their results that the strengthening of the thermal gradients in the LGM (relative to the base period) simulations do not cause an increase in precipitation (at the fronts) and that overall there is less precipitation in the extratropical cyclones (for clear physical reasons, which are stated). The high-resolution model data is also useful for reaching their conclusions as they do not have to make inferences from other (statistical) downscaling methods.

The cyclone composites also clearly show the increase in wind speed and lower precipitation associated with these systems and therefore the authors reach the logical conclusion that the increased cyclone activity, combined with stronger low-level winds and lower precipitation, are likely to be responsible for the frequent dust storms the proxy data suggest. The manuscript is well written, provides a logical sequence of evidence and draws sound conclusions from them. The paper would be a good addition to the literature and should encourage other similar analyses for other models/epochs. I do have a fairly large number of minor points that should be considered, but they should be very straightforward to address.

Answer: We want to thank the Reviewer for the thorough examination and positive assessment of our manuscript. We reply point-by-point to the Reviewer's comments or give detailed arguments about our reasoning for those cases in which we did not follow a Reviewer suggestion. Our responses are shown in red colour. Text from the manuscript is identified by quotation marks and italic font style, added or modified text can be identified by colour.

## SPECIFIC POINTS

Important note: In case no specific answer can be found below a comment, we have simply implemented the suggested text changes as requested.

Line 19/20: “. . .which is typically. . .” change to “. . .which are typically. . .”

End of line 37: change stronger to larger (“larger differences” reads better).

Lines 41-42: Re-word to something more concise like, “One important issue preventing non-recent or non-21st century cyclone analysis is the availability of climate model output with sufficient spatial and temporal resolution to enable identification, tracking and characterisation of such cyclones.”

Line 56: Change “enhanced” to “stronger”.

Lines 57-58: change to: “. . .leading to a southward displaced, more intense and less variable North Atlantic jet than under. . .”

Line 59: change “related with” to “related to”.

Lines 68-71: the sentence starting “For example,” in line 68 is too long and I struggled to make sense of it. Please would you break it up into two sentences and re-word it.

A: we have changed the sentence as follows:

*“For example, Ludwig et al (2017) **implemented** more realistic boundary conditions **in terms of the** North Atlantic SSTs, land use types and vegetation cover **in a regional climate model (RCM) to simulate the regional climate under LGM conditions. Their results in terms of LGM temperature, precipitation and the permafrost margin are in better agreement with the proxies than without the implemented boundary conditions.” (line 74ff)***

Line 66: insert “the” before “LGM in PMIP3”.

Whole paragraph, lines 56-74: There is this paper (below) that suggests reduced storminess over the North Atlantic at the LGM, which the authors should consider as a counter-view to their paper. It does not invalidate the results here whatsoever, but does provide an important (and perhaps opposing) view of the North Atlantic at the LGM. Just a sentence acknowledging this and citing the paper would be sufficient: Rivière, G., S. Berthou, G. Lapeyre, and M. Kageyama, 2018: On the Reduced North Atlantic Storminess during the Last Glacial Period: The Role of Topography in Shaping Synoptic Eddies. J. Climate, 31, 1637– 1652, <https://doi.org/10.1175/JCLI-D-17-0247.1>

A: we thank the reviewer for his comment and the reference, which we have implemented in the text and shortly discussed. Additional comments from M. Löffverström (SC1) were also included.

*“Under the influence of the continental ice sheets and extended sea ice, the PMIP3 GCMs show stronger meridional temperature gradients, leading to a southward displaced, more intense and less variable North Atlantic jet than under current climate conditions (Löffverström et al, 2014; 2016; Merz et al., 2015; Wang et al. 2018). These differences have been related e.g., to more dominant cyclonic Rossby wave breaking near Greenland (Rivière et al., 2010), stationary wave packets trapped in the mid-latitude wave guide (Löffverström, 2020) and to enhanced meridional eddy momentum flux convergence over the North Atlantic (Wang et al., 2018). In line with a southward displaced and stronger jet stream, several studies show a more intense and southward shifted North Atlantic storm track compared to today’s climate (e.g., Hofer et al., 2012; Luetscher et al., 2015; Ludwig et al., 2016). However, other studies display reduced storm track activity over the North Atlantic in spite of the enhanced baroclinicity (e.g. Donohoe and Battisti, 2009; Rivière et al., 2010; Löffverström et al., 2016). Rivière et al. (2018) discusses a reduced baroclinic conversion as a possible reason for this apparent discrepancy, arguing that the eddy heat fluxes are less well aligned with the mean temperature gradient for LGM than for PI. Other arguments for the reduced storminess include model resolution, parameterizations and boundary conditions (e.g. Donohoe and Battisti, 2009; Rivière et al., 2018). Thus, the intensity differences between LGM and PI North Atlantic storm track activity may be model dependent.” (lines 56ff).*

Line 78: change to “. . .compared to their modern counterparts at high spatial. . .”.

Line 84: change to “. . .our analysis is data from the third phase. . .”

Lines 87-88: change “adapted” to “lower” as the greenhouse gas concentrations are lower.

Line 90: Remove the “have” after the Ludwig et al. (2016) reference.

Line 91: Include “the” before “LGM”.

Line 92: Change to “. . .slightly different jet structure to some of the other. . .”

Lines 92-93: remove the words, “in terms of the difference between PI and LGM conditions” as they unnecessarily make the sentence too long.

Lines 108-109: change to “. . .to simulate the TOP 30 cyclones (from PI and LGM) with a grid spacing of. . .”

Lines 112-114: Different spellings of parametrisation/parametrization – make sure you are consistent (either way seems OK with Copernicus Publications but you need to be consistent – see manuscript preparation guidelines).

Line 112: Change to “An overview of the parametrisation choices is given in Table 2.” As it is more concise.

Paragraph for lines 119-126: Start the paragraph with something like, “The TOP 30 cyclone tracks simulated by WRF were identified manually. . .”. Just to be clear that you have not manually tracked all cyclones in these simulations.

Line 121: Change “equally” to “each”.

Line 123: Change “For the sake of succinctness,” to “For brevity,”.

Line 124: Change “The here analysed target variables based on the 12.5. . .” to “The variables analysed from the 12.5. . .”.

Lines 130-131: I think you should actually include the plot of MPI-ESM-P vs reanalyses in the paper to help this section. It makes it quicker and easier for the reader to verify your statement. Including the figure in the supplement would be absolutely fine.

A: We thank the reviewer for this suggestion. As requested, we have added a further figure to the supplementary material showing the difference between MPI-ESM-P (PI and LGM) and the NCEP/NCAR reanalyses (Figure S1 +S2) and added a short notice at the beginning of chapter 3.

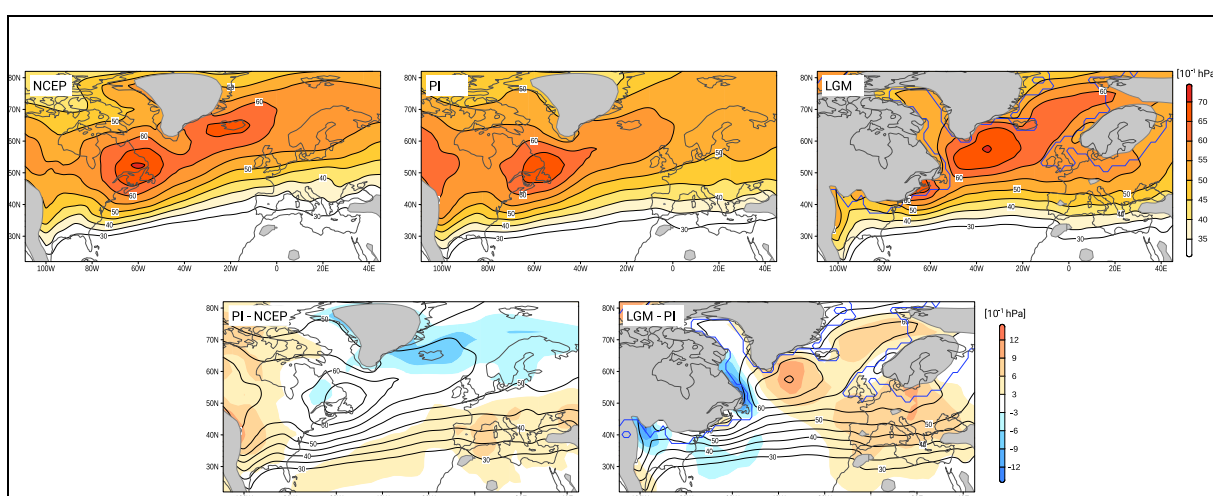


Fig. S1: Top: storm tracks (2–6 days band passed filter of daily MSLP data [ $1/10$  hPa]) for the NCEP Reanalysis data and the MPI-ESM-P simulations for PI and LGM. Bottom: differences (shaded) between PI (lines) and NCEP and between LGM (lines) and PI. Areas with topography higher 1000 m shaded grey, LGM ice sheet extent marked by the blue line.

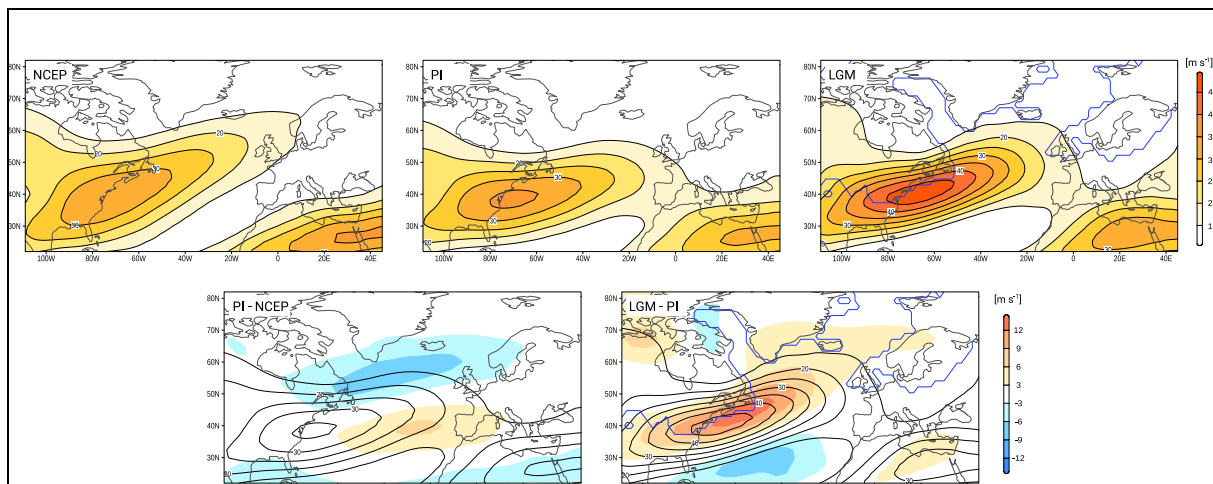


Fig. S2: Top: Upper level jet stream (wind speed at 300 hPa [m/s]) for the NCEP Reanalysis data and the MPI-ESM-P simulations for PI and LGM. Bottom: differences (shaded) between PI (lines) and NCEP and between LGM (lines) and PI. LGM ice sheet extent marked by the blue line.

“Figure 2 shows the cyclone track density for the extended winter for PI and LGM climate conditions. In spite of the lower spatial resolution of MPI-ESM-P, the cyclone track density for the PI is close to cyclone statistics obtained with Reanalysis datasets, *with slight southerly shift of cyclonic activity (see Figure S1 for comparison with NCEP reanalysis data (Kalnay et al, 1996)), and CMIP GCMs for recent climate conditions (cp. Pinto et al., 2007; their Figure 1). Still, some regional shortcomings are identified, notably the limited cyclone activity over the Mediterranean basin. The North Atlantic storm track shows a clear tilt towards Northern Europe and the Arctic Ocean for PI, and its location and orientation are closely related with the eddy-driven jet stream (black contours in Fig. 2a) and the associated upper-air baroclinicity (Hoskins and Valdes, 1990; Pinto et al., 2009). A comparison of the jet stream between MPI-ESM-P PI and NCEP Reanalysis data shows a slight tilt towards Europe by the MPI model (Fig. S2), in line with the enhanced (reduced) southward (northward) cyclone activity (Fig. S1)“ (lines 136ff)*

Lines 136-137: Change “The North Atlantic storm track looks quite different under LGM conditions: the cyclone track density is strongly enhanced over the North Atlantic and more constraint along a corridor close to the ice edge (Fig. 2b).” to “The North Atlantic storm track looks quite different under LGM conditions relative to PI: the cyclone track density is higher over the North Atlantic and more constrained to the ice edge (Fig. 2b).”

Line 142: I read the numbers 12.071 vs. 9.541 as “twelve versus nine-and-a-half” cyclones over a 30 year period. Is this supposed to be 1000 times that i.e. twelve and nine thousand, respectively over a 30 year period? That would be about 2.2/day vs. 1.8/day, which seems

right. If it is 'thousands' of cyclones then just put 12071 and 9541 as the inclusion of the decimal point could mean different things to different readers and removing it would remove any confusion.

A: we agree the text was not very clear, and has been changed as follows:

*"For the North Atlantic (70°W – 0°, 35°N – 70°N), the total number of cyclones for the analysed 30-year period is about 26% larger for LGM than for PI conditions (12071 vs. 9541 individual cyclone counts in 30 years, corresponding to roughly 2.2 cyclones/day vs 1.8 cyclones/day)." (lines 151ff)*

Line 144: add 'the' here, "for the LGM"

Line 146: change "cyclogenesis is enhanced" to "the rate of cyclogenesis has increased". I find the use of "enhanced" can be ambiguous. Do you mean the cyclones deepen faster? More cyclones generated? Other features associated with cyclogenesis strengthen? Stating that the number of storms being formed has increased (instead of enhanced) makes the sentence much clearer. Please consider the use of "enhanced" elsewhere and whether a more direct statement can be made (as above).

Line 146: regarding enhanced. . . you could say, "On the other hand, there is more cyclolysis along the borders. . .". Again, what aspect of cyclolysis is "enhanced"? If you mean more storms are decaying there then you can just use the suggested wording above.

Line 147: Change "in strong deviation" to "relative".

Line 149: remove the word "reveal" and replace with "have".

Line 152: remove "particularly".

Line 153: do you mean ice sheets not shields?

Lines 153-154: Sentence starting "This is in strong. . ." does not seem to quite make sense to me and I am not sure how to re-word it. Could you check to make sure it is clearly stating what you want it to say.

A: We thank the reviewer for pointing this out, we agree that the wording was not clear, and that this sentence kind of duplicates what is said in the previous sentence. We have deleted the sentence, and slightly changed the previous sentence.

*“Deepening rates are stronger for LGM cyclones over the central north Atlantic, as well as their filling rates close to the ice edge / ice sheets (Fig. 3g,h).” (lines 163ff)*

Line 158: “LGM cyclones are on average more intense than their PI counterparts”. While I accept this is true, your analysis/summary of the figure does not clearly show this. All I can see is a skewed distribution. You just need to quantify this and then quote the mean (and median, given the distribution shape) in the text to back this statement up.

A: Thanks for this, we have added the numbers to the text.

*“Figure 4 displays the relative frequency distribution of the cyclone intensity over the North Atlantic area (70°W – 0°, 35°N – 70°N), revealing that LGM cyclones are on average more intense (mean (median): 1.58 (1.41) hPa deg. lat.<sup>-2</sup>s<sup>-1</sup>) than their PI counterparts (mean (median): 1.43 (1.28) hPa deg. lat.<sup>-2</sup>s<sup>-1</sup>).” (lines 167ff)*

Line 169: Again, quote the actual mean/median value from the cyclones in Table 3 to clearly show that the vorticity is higher for the LGM relative to PI.

A: Again, we added the numbers to the text (see above). Additionally, we added a line to the table including mean/median values for better comparison.

*“LGM extreme cyclone trajectories are more zonally orientated and constrained to a narrower corridor (particularly until 15°W) than their PI counterparts, and they achieve higher vorticity (mean Laplacian of MSLP for LGM: 2.80; PI: 2.52) values during lifetime (Tab. 3).” (lines 177ff)*

Line 188: Change “Take” to “Taking”.

Line 193: Change to “. . . temperature at 850 hPa for LGM relative to PI”.

Line 194: Change “apparently faster” to “displaced forward in the cyclone”.

Line 200: Change “for LGM extremely cyclones” to “for the LGM extreme cyclones”

Line 202: Change “strongly increased” to “much higher”.

Line 203: Change m/s to m s<sup>-1</sup>.



Line 213: Change “occurring climate” to “climatic conditions”.

Line 214: Change “under LGM conditions” to “at the LGM”.

Line 229: Just say “shortcomings” not “some shortcomings”, also give an example the sort of shortcoming you are referring to.

Line 230: Change “this caveat” to “those shortcomings”.

Line 231: Change “Pfahl et al. (2015) had” to “Pfahl et al. (2015) has”.

Lines 234-239: Sentence starting “Even though. . .” is far too long and needs to be broken into at least two sentences.

A: We agree the sentence was too long and have broken it into two separate sentences

*“Even though lower cyclone-related precipitation may be partially compensated by the moisture advection embedded in the (stronger) westerly large-scale flow, particularly for areas where orographic precipitation dominates (e.g. upward slopes of mountain ranges / glaciers), it is consistent with the hypothesis of a drier Western and Central Europe. The view of a drier Europe is also consistent with the dominant land cover types estimated from proxy data (Ray and Adams, 2001) or a statistical reconstruction based on temperature and precipitation (Shao et al., 2018), namely polar desert close to the glaciers, forest steppe over Southern Europe and steppe in-between.” (line 245ff)*

Line 240: change to “close to the Iberian Peninsula for cyclone selection leads. . .”.

Line 243: add ‘the’ – “typically initiated by the wind. . .”.

Line 246: change to “have been stronger than at present. . . (Maher. . .)”.

Line 247: Change “document of a past when” to “indicate that”

Line 250: What’s an “adequate large-scale circulation”? Do you mean, “stronger largescale flow”?

A: Yes, this is what we meant, text changed (line 259)

Line 255: remove “European” as you state Europe at the start of the sentence.

Line 257-258: change to “. . .individual LGM cyclones could trigger such dust. . .”.

Line 258: Change “strong wind speeds” to just “strong winds”.



Line 259: change to “. . .trigger dust emission and transport over short. . .”.

Line 260-261: sentence starting “As the precipitation. . .” was confusing. You need to say something like, “As moisture acts to make surface dust particles more cohesive (REFERENCE\*), the reduced cyclone precipitation and higher wind speeds in LGM cyclones would have actually been more conducive to generating dust storms” – or something close to those words. \*please find and insert an appropriate reference here.

A. Thanks for the suggestion, implemented as suggested:

*“As moisture acts to make surface dust particles more cohesive (e.g., Ishizuka et al., 2008), the reduced cyclone precipitation and higher wind speeds in LGM cyclones would have actually been more conducive to generating dust storms.” (lines 270ff)*

Line 273: change “featuring an enhanced number and” to “featuring more frequent and intense” which is much clearer.

Lines 276-277: Change “LGM cyclones were more intense due to stronger baroclinicity and apparently less influenced by diabatic processes (lower rainfall, lower temperatures, lower water vapour content).” to “LGM cyclones were more intense due to stronger baroclinicity with less influence from diabatic processes (lower rainfall and lower water vapour content).”

Note: I removed ‘lower temperature’ as temperature can change adiabatically, which matters given e.g. lower sea levels and therefore higher mean sea level pressure, which would affect temperature.

Line 293: change “in favour of an extended used” to “for the extended use”.

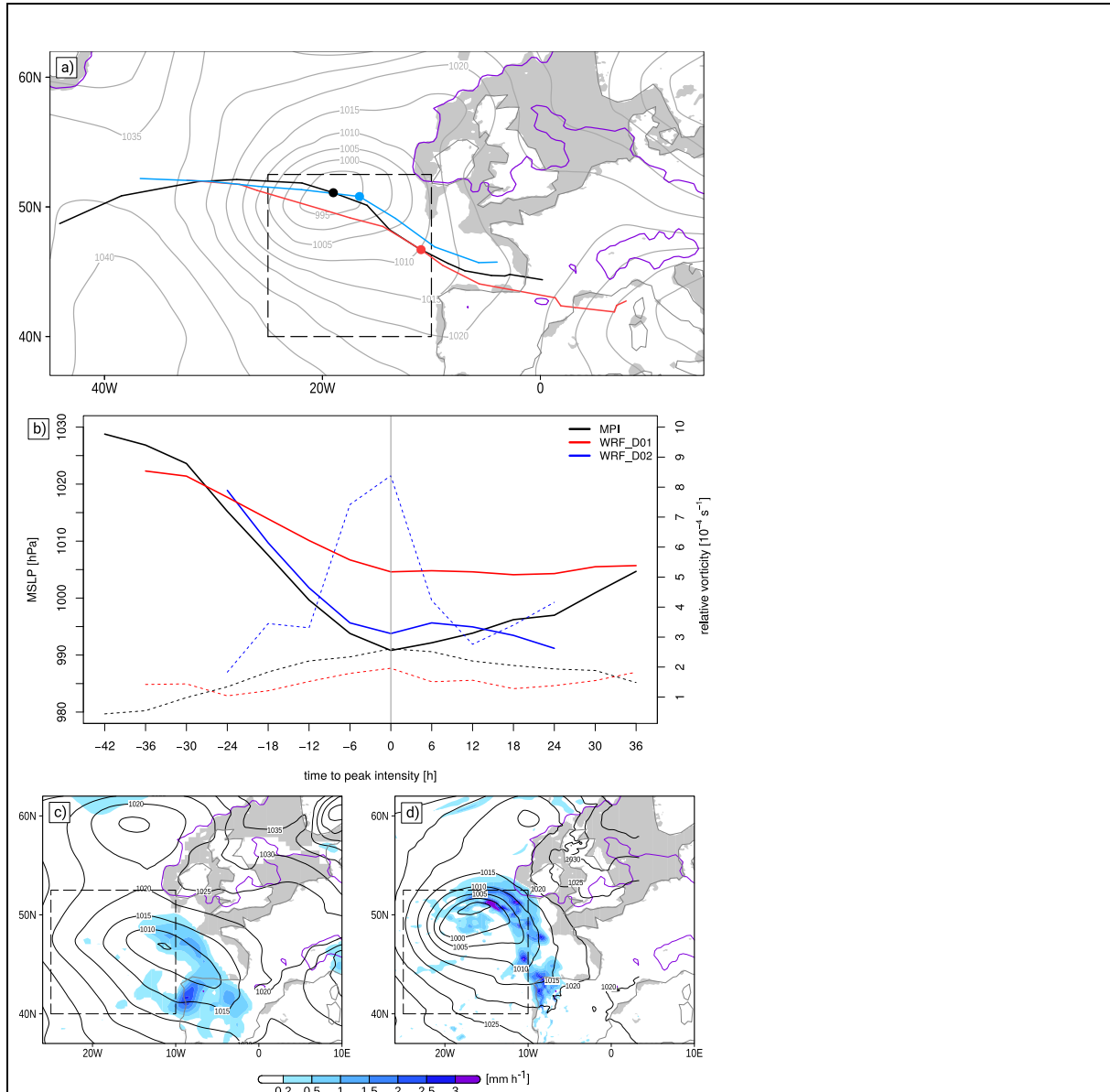
Figure 1 caption: change “extends” to “extents”.

Figure 3 caption: change “. . .ice sheet extends marked by blue line. . .” to “ice sheet extents marked by the blue line. . .”.

Figure 4 caption: change “. . . the y-axis is zoomed in.” to “. . .the y-axis is adjusted (right figure).”

Figure 6: the MSLP in WRF 12.5 Fig. 6(d) is lower at the cyclone centre than WRF 50's cyclone centre in Fig. 6(c) but the MSLP is higher (and not even below 990 hPa, whereas I can see a 985 hPa closed contour in Fig. 6d) in the WRF 12.5 km than either of the other two models. This does not look correct. Please check this as the MSLP changes in Fig 6(b) would not be consistent with the vorticity changes given the method of calculating vorticity.

A: Thanks for pointing this out. There were wrong settings to the axes handling in the plotting script which has been corrected. The MSLP changes are now consistent with the changes in vorticity. See updated figure below:



*“Figure 6. Comparison of (a) cyclone tracks for MPI-ESM (black), WRF 50km (red) and WRF 12.5 km (blue) (coloured dots mark the location of peak intensity, black dotted box shows target area) and MSLP [hPa] for MPI-ESM at peak intensity, (b) timeseries of cyclone core pressure and relative vorticity for MPI-ESM, WRF 50km and WRF 12.5 km for LGM cyclone #24. Simulated precipitation rate [mm h<sup>-1</sup>] (shaded) and MSLP [hPa] (lines) at peak intensity for (c) WRF 50km and (d) WRF 12.5km.”*

Figure 7: The caption is incorrect. Where you refer to (d, e) and (f – g) I think you mean (d – f) and (g – i). Please re-read the caption carefully and make sure it corresponds to the correct figure panels. Also, you refer to the ‘field mean’ in the caption – averaged over what area? The cyclone area? Hemisphere? Globe? Please be clear on that.

Figure S1: The same issue as described for the Figure 7 caption applies to this figure too. Please check through it.

A: We have reworded the captions in both Fig. 7 and S3 (former Fig. S1) and added information about the field mean (which is the mean over the displayed area).

*“Figure 7. Composites of (a - c) mean sea level pressure, (d - f) ThetaE, and (g - i) vertical integrated water vapour (IWV) for PI, LGM and difference LGM – PI at peak intensity as defined by the maximum of the Laplacian of MSLP. (a, b) absolute MSLP values (lines, [hPa]), anomalies [hPa] from mean over displayed area (coloured); (c) absolute MSLP values (lines, [hPa]) from LGM, differences of the anomalies between LGM – PI in colours; (d, e) absolute ThetaE values (lines, [K]) and anomalies [K] from mean over displayed area (coloured); (f) absolute ThetaE values (lines, [K]) from LGM, differences of the anomalies between LGM – PI in colours; (g, h) absolute IWV values [mm], (i) difference [mm] LGM – PI.”*

## Replies to Anonymous Referee #2

Original comments received and published: 6 January 2020

This is an interesting paper assessing how cyclone activity differed in parts of the northern hemisphere during the last glacial maximum. The paper is well written and the results are interesting, particularly the cyclone composites from the regional model simulations showing the different cyclone impacts between the two periods.

Answer: We want to thank the Reviewer and the Editor for the thorough examination and positive assessment of our manuscript. We reply point-by-point to the Reviewer's comments or give detailed arguments about our reasoning for those cases in which we did not follow a Reviewer suggestion. Our responses are shown in red color. Text from the manuscript is identified by quotation marks and italic font style, added or modified text can be identified by red color.

My major comment is that the ice sheets and sea level change resulted in quite substantial differences in topography, MSLP etc between the two periods, which influences how the tracking scheme functions. I think there would be a great deal of value in using a higher level in the atmosphere (e.g. 500hPa) for identifying cyclones to assess how robust the observed changes are. I recognise that this is difficult (due to the time involved) or possibly impossible, depending on what data exists for the global model, but it could provide some useful insights, even just from the WRF simulations.

A: we thank the reviewer for this suggestion. As the reviewer correctly assumes, it would be very time consuming and in our opinion little informative to perform the tracking of cyclones at 500 hPa within the scope of this manuscript. Cyclones are typically tracked based on surface or near-surface fields, e.g. MSLP or relative vorticity at 850 hPa geopotential height (see Neu et al., 2013 for a description and comparison of many methodologies). In fact, the 500 hPa geopotential height field does not typically feature closed pressure systems, but rather troughs and ridges. In line with the reviewers suggestions, we thought about preparing an additional figure showing the 500 hPa storm track field for the reanalysis, PI and LGM conditions. The storm track shows the variance of the 500 hPa geopotential height within the synoptic scale and is this a measure of synoptic activity (Hoskins and Valdes, 1990). Unfortunately, no 6-hourly nor even daily pressure level data is available in the PMIP3 database. This is why we have estimated the storm track in Ludwig et al. (2016) based on the MSLP fields (here also used for the cyclone tracking, see new Fig. S1). While a conversion between the MPI-ESM-P data from model levels to pressure levels is possible in

principle, we have refrained from taking this path as we expect little added information compared to the MSLP storm track (Ludwig et al., 2016) and cyclone track information (here)

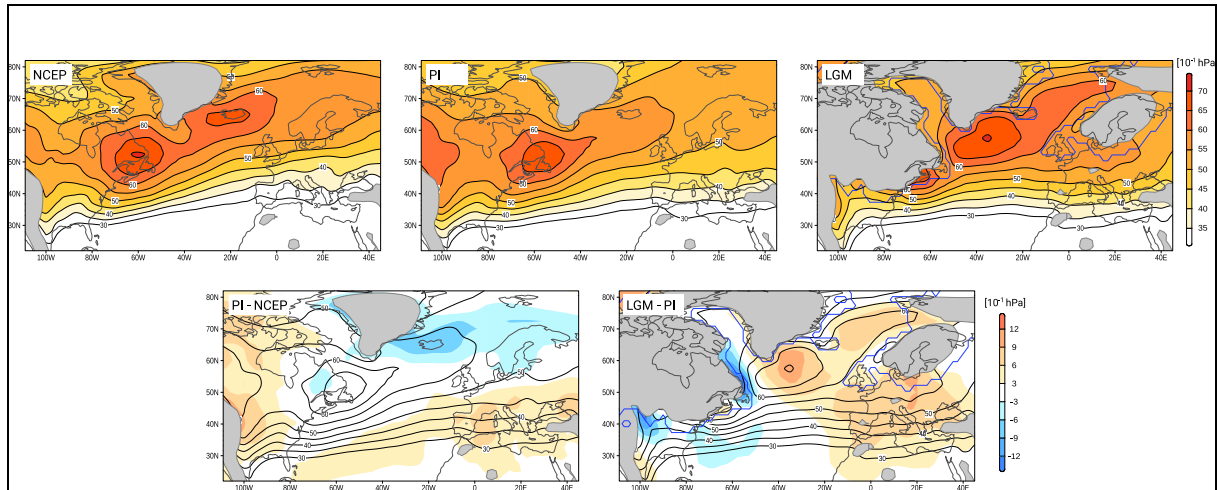


Fig. S1: Top: storm tracks (2–6 days band passed filter of daily MSLP data [ $1/10$  hPa]) for the NCEP Reanalysis data and the MPI-ESM-P simulations for PI and LGM. Bottom: differences (shaded) between PI (lines) and NCEP and between LGM (lines) and PI. Areas with topography higher 1000 m shaded grey, LGM ice sheet extent marked by the blue line.

We agree with the reviewer that looking at the vertical structure of the cyclones (see Dacre et al., 2012; their Fig. 4 <https://doi.org/10.1175/BAMS-D-11-00164.1>) in WRF for LGM and PI conditions would be very interesting. While we think this does not fit well with the scope of the present study, we will surely look into this in the future.

Minor comments:

L89 - I would appreciate more information on why this specific global model was chosen, especially as you say its large-scale circulation is different from other models. Please also note its spatial resolution.

A: We are based in Germany and we had access via the DKRZ to the 6-hourly 3D MPI-ESM-P fields. These served as boundary conditions for the WRF simulations. Please note that the surface and atmospheric fields stored on the PMIP3 database are not sufficient to serve as boundary conditions for a regional climate model. Theoretically, we could ask each modelling group for the high resolution 3D-data and re-do the current analysis in case the needed data is available. This is one of the reasons we state in the conclusions that the analysis should be expanded based on other GCMs (and also RCMs) to confirm (or not) the current results.

We now indicate in the text that the choice of GCM was largely motivated by the data availability.

*“This choice was motivated by the availability of six hourly 3-D model level data needed for running the RCM.” (line 97)*

L119 - does identifying cyclones manually make much difference compared to the tracking scheme used for the GCM cyclones?

A: The tracking scheme applied to the GCM data is fully automatic (Murray and Simmonds, 1991; Pinto et al., 2005) and widely used in the community (see e.g. review paper Neu et al 2013). These tracking schemes are optimised to process enormous amounts of data but with a rather low spatial and time resolution (e.g. 6-hourly, T63-data). For the RCM data, there was no need to use such a tracking method, particularly if only a very small amount of cyclones is analysed (TOP 30 for LGM and PI) and the spatial and time resolutions was very high (12.5 km, hourly). Given that the performance of the tracking methods typically increases with higher spatial and particularly time resolution, we assume that the results using a comparative tracking method would be similar to our manual analysis. Following one of the suggestions by the first reviewer, we now clearly indicate that the manual tracking was only performed for 2x 30 cyclones.

*“The TOP 30 cyclone tracks simulated by WRF were identified manually based on relative vorticity field at 850 hPa.” (line 126)*

L130 - I would appreciate some more evaluation of how the model compares to reanalyses included within this paper.

A: We thank the reviewer for this suggestion. Also following a comment by the first reviewer, we have added a notes to the first and second paragraph of chapter 3 and two additional supplementary figures (Fig. S1, S2) comparing the storm track and the upper level jet stream in the MPI-ESM-P model for PI and LGM conditions and the NCEP/NCAR reanalysis.

*“Figure 2 shows the cyclone track density for the extended winter for PI and LGM climate conditions. In spite of the lower spatial resolution of MPI-ESM-P, the cyclone track density for the PI is close to cyclone statistics obtained with Reanalysis datasets, with slight southerly shift of cyclonic activity (see Figure S1 for comparison with NCEP reanalysis data (Kalnay et*

al, 1996)), and CMIP GCMs for recent climate conditions (cp. Pinto et al., 2007; their Figure 1). Still, some regional shortcomings are identified, notably the limited cyclone activity over the Mediterranean basin. The North Atlantic storm track shows a clear tilt towards Northern Europe and the Arctic Ocean for PI, and its location and orientation are closely related with the eddy-driven jet stream (black contours in Fig. 2a) and the associated upper-air baroclinicity (Hoskins and Valdes, 1990; Pinto et al., 2009). A comparison of the jet stream between MPI-ESM-P PI and NCEP Reanalysis data shows a slight tilt towards Europe by the MPI model (Fig. S2), in line with the enhanced (reduced) southward (northward) cyclone activity (Fig. S1)” (line 136ff)

Figure S1 (see above) reply to major concern

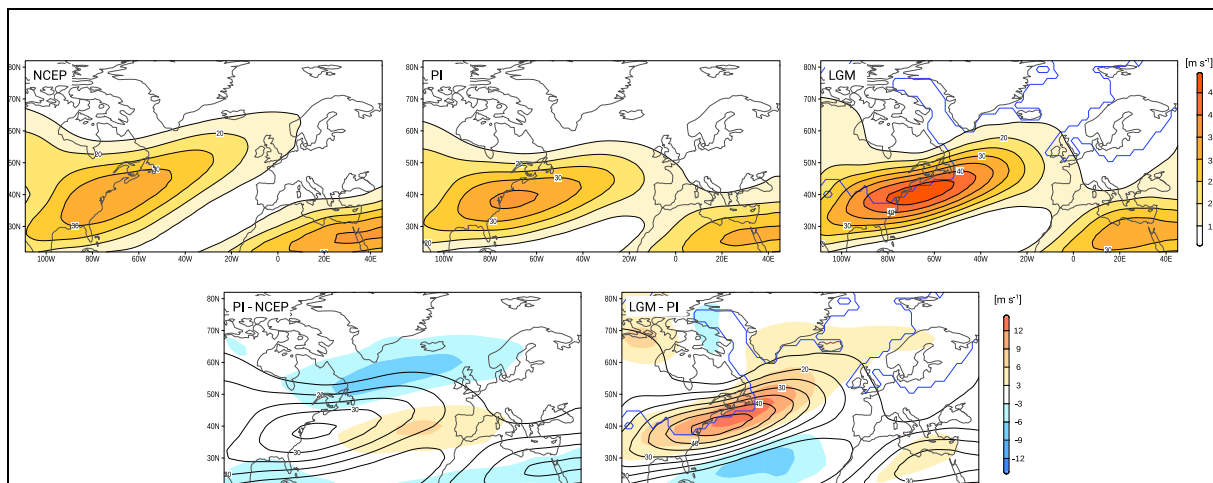


Fig. S2: Top: Upper level jet stream (wind speed at 300 hPa [m/s]) for the NCEP Reanalysis data and the MPI-ESM-P simulations for PI and LGM. Bottom: differences (shaded) between PI (lines) and NCEP and between LGM (lines) and PI. LGM ice sheet extent marked by the blue line.

L173 - please elaborate on how “care was taken” that the tracks align. It would be nice to see some statistics comparing e.g. mean biases in location/intensity, rather than just for a selected cyclone.

A: We have carefully analysed all 60 selected cases to make sure that the GCM and RCM tracks are consistent in terms of the initial location, track and timing, i.e. that we are analysing the same cyclone. The intensity in terms of Laplacian of MSLP is not comparable between RCM and GCM data because of the different spatial resolution.



Table 3 - In addition (or instead of) these stats for all cyclones, some summary statistics of the top 30 cyclones for each simulation would be helpful. E.g. mean intensity and cyclogenesis latitude from the GCM, or mean wind speed, rain rate, etc from the WRF simulations.

A: We thank the reviewer for this suggestion. Some mean statistics have been included for the GCM in Table 3 (see additional lines at the bottom). Since we only consider cyclones with peak intensity inside the box, the cyclone longitude/latitude is almost similar for PI and LGM. However, the mean/median of the intensity shows enhanced values for LGM cyclones. For the WRF-Simulations, we added an additional table (S1) in the supplementary showing mean (maximum) wind speed / rain rate, 12 hours before/ after and at peak intensity for PI and LGM (to be consistent with Fig.8, Fig. S4, Fig. S6) for comparison.

Table 3, only additional lines

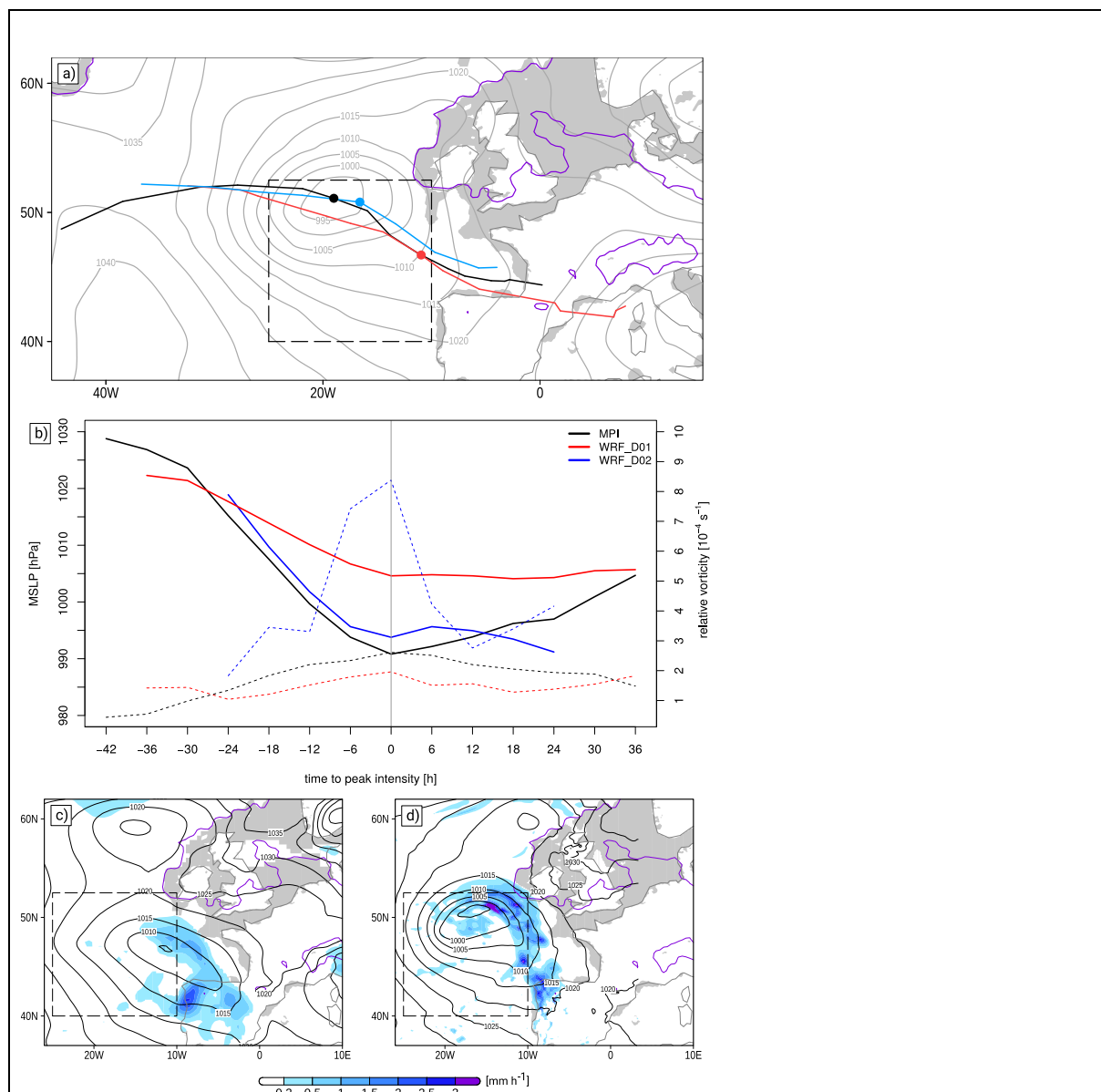
| PI |       |      |        |       |        | LGM  |      |        |       |        |
|----|-------|------|--------|-------|--------|------|------|--------|-------|--------|
|    | Date  | Time | Lapl P | °Lat  | °Lon   | Date | Time | Lapl P | °Lat  | °Lon   |
|    | Mean  |      | 2.52   | 47.51 | 342.72 |      |      | 2.80   | 48.53 | 342.53 |
|    | Media |      | 2.49   | 47.59 | 343.56 |      |      | 2.73   | 49.76 | 343.54 |

Table S1: Summary of wind speed at 925 hPa, maximum near surface wind gust and total precipitation of the TOP 30 PI and LGM ensemble with 12.5 km resolution for 12 hours before / after and at peak intensity. Field mean and maximum corresponds to area depicted in Fig. S4, Fig. S6 and Fig. 8.

|     | wind925 (mean) [m/s] |       | wind925 (max) [m/s] |       | VMAX (mean) [m/s] |       | VMAX (max) [m/s] |       | PREC (mean) [mm/h] |      | PREC (max) [mm/h] |      |
|-----|----------------------|-------|---------------------|-------|-------------------|-------|------------------|-------|--------------------|------|-------------------|------|
|     | PI                   | LGM   | PI                  | LGM   | PI                | LGM   | PI               | LGM   | PI                 | LGM  | PI                | LGM  |
| -12 | 9.56                 | 11.37 | 24.71               | 27.23 | 12.46             | 14.10 | 23.04            | 25.24 | 0.29               | 0.20 | 3.45              | 2.05 |
| 0   | 10.67                | 12.25 | 25.96               | 27.95 | 13.47             | 15.49 | 26.84            | 26.98 | 0.28               | 0.24 | 3.56              | 2.70 |
| 12  | 11.69                | 12.91 | 26.68               | 28.82 | 14.50             | 16.09 | 28.66            | 30.31 | 0.24               | 0.24 | 1.66              | 1.27 |

Figure 6 c/d - it would be nice to have an additional panel showing the MSLP field in the GCM

A: The MSLP field from the GCM was included in Fig. 6a for comparison. Thus, now the MSLP fields are shown for the GCM, WRF-50km and WRF12.5km. Following a comment by the first reviewer, a bug in Fig. 6b was also corrected.



“Figure 6. Comparison of (a) cyclone tracks for MPI-ESM (black), WRF 50km (red) and WRF 12.5 km (blue) (coloured dots mark the location of peak intensity, black dotted box shows target area) and MSLP [hPa] for MPI-ESM at peak intensity, (b) timeseries of cyclone core pressure and relative vorticity for MPI-ESM, WRF 50km and WRF 12.5 km for LGM cyclone #24. Simulated precipitation rate [mm h<sup>-1</sup>] (shaded) and MSLP [hPa] (lines) at peak intensity for (c) WRF 50km and (d) WRF 12.5km.”

Figure 7 - are the differences in panels c and f between the absolute values or between the anomalies? Given that there is the large mean MSLP difference between the simulations, I think the difference in local anomalies might be more informative for understanding how e.g. pressure gradients differ between simulations.

A: Based on the comment, we agree that the caption was not clear enough. Panels c and f indeed show differences of the anomalies (in line with the reviewers' suggestions), which is now clearly stated in the Figure caption.

*“Figure 7. Composites of (a - c) mean sea level pressure, (d - f) ThetaE, and (g - i) vertical integrated water vapour (IWV) for PI, LGM and difference LGM – PI at peak intensity as defined by the maximum of the Laplacian of MSLP. (a, b) absolute MSLP values (lines, [hPa]), anomalies [hPa] from mean over displayed area (coloured); (c) absolute MSLP values (lines, [hPa]) from LGM, differences of the anomalies between LGM – PI in colours; (d, e) absolute ThetaE values (lines, [K]) and anomalies [K] from mean over displayed area (coloured); (f) absolute ThetaE values (lines, [K]) from LGM, differences of the anomalies between LGM – PI in colours; (g, h) absolute IWV values [mm], (i) difference [mm] LGM – PI.”*

## Replies to Short Comment #1

Marcus Lofverstrom (lofverstrom@arizona.edu)

Original comments received and published: 6 January 2020

I really enjoyed reading this manuscript and I hope the review process will be smooth. I have two small comments/requests though:

Answer: We want to thank the Colleague for his comments to our manuscript. We reply point-by-point to the Reviewer's comments. Our responses are shown in red color. Text from the manuscript is identified by quotation marks and italic font style, added or modified text can be identified by red colour.

(1) This manuscript was recently accepted for publication in EPSL. Among other things, it presents a new interpretation of the LGM jet zonalization in the N Atlantic and the precipitation distribution in SW Europe. I would greatly appreciate if the authors could cite this paper when you discuss these topics in the introduction. Link to accepted manuscript:

<https://authors.elsevier.com/a/1aRAS.lq4KpRO>

A: We thank the colleague for this suggestion. We now included a reference to this paper in the introduction (line 60, see text in next reply).

(2) The main result of the present study is at odds with a number of GCM studies that, contrary to findings here, show a reduced storminess in the N Atlantic at the LGM. It would be good to add a paragraph in the discussion section that puts these contrasting results in perspective with one another, and if possible, provide at least a speculative interpretation of possible sources of this discrepancy. For example, it could be model dependent (the top three studies used CCSM3 derivatives, and Riviere et al used IPSL), resolution could be a factor (this paper discussed this aspect in some detail in GCM simulations – see e.g. Fig 1: <https://www.the-cryosphere.net/12/1499/2018/tc-12-1499-2018.html>), parameterizations, boundary conditions (again, top three studies used PMIP2 boundary conds.), etc.

Li and Battisti, 2008 JCLim <https://journals.ametsoc.org/doi/full/10.1175/2007JCLI2166.1>

Donohoe and Battisti, 2009 JCLim

<https://journals.ametsoc.org/doi/full/10.1175/2009JCLI2776.1>

Lofverstrom et al. 2016 JAS <https://journals.ametsoc.org/doi/full/10.1175/JAS-D-15-0295.1>

Riviere et al, 2018, JCLim <https://journals.ametsoc.org/doi/full/10.1175/JCLI-D-17-0247.1>

A: We also thank the colleague for this suggestion. A similar comment had been posted by reviewer #1. We have enhanced our discussion on this issue and explicitly state that the changes in storminess in the PMIP3 models depends on the model choice, parameterizations and chosen boundary conditions.

*“Under the influence of the continental ice sheets and extended sea ice, the PMIP3 GCMs show stronger meridional temperature gradients, leading to a southward displaced, more intense and less variable North Atlantic jet than under current climate conditions (Löfverström et al, 2014; 2016; Merz et al., 2015; Wang et al. 2018). These differences have been related e.g., to more dominant cyclonic Rossby wave breaking near Greenland (Rivière et al., 2010), stationary wave packets trapped in the mid-latitude wave guide (Löfverström, 2020) and to enhanced meridional eddy momentum flux convergence over the North Atlantic (Wang et al., 2018). In line with a southward displaced and stronger jet stream, several studies show a more intense and southward shifted North Atlantic storm track compared to today’s climate (e.g., Hofer et al., 2012; Luetscher et al., 2015; Ludwig et al., 2016). However, other studies display reduced storm track activity over the North Atlantic in spite of the enhanced baroclinicity (e.g. Donohoe and Battisti, 2009; Rivière et al., 2010; Löfverström et al., 2016). Rivière et al. (2018) discusses a reduced baroclinic conversion as a possible reason for this apparent discrepancy, arguing that the eddy heat fluxes are less well aligned with the mean temperature gradient for LGM than for PI. Other arguments for the reduced storminess include model resolution, parameterizations and boundary conditions (e.g. Donohoe and Battisti, 2009; Rivière et al., 2018). Thus, the intensity differences between LGM and PI North Atlantic storm track activity may be model dependent.” (lines 56ff).*

In the discussion, we have added:

*“Given that this study is based on a single GCM, a single tracking method and a single RCM, it should be regarded as a preliminary analysis as the uncertainties of the jet stream position and storm track activity (e.g., Merz et al, 2013, Riviere et al., 2018) may be considerable among different GCMs.” (lines 293ff)*

# Extratropical cyclones over the North Atlantic and Western Europe during the Last Glacial Maximum and implications for proxy interpretation

Joaquim G. Pinto<sup>1</sup> and Patrick Ludwig<sup>1</sup>

5 <sup>1</sup>Institute of Meteorology and Climate Research, Karlsruhe Institute of Technology, 76131 Karlsruhe, Germany

*Correspondence to:* Joaquim G. Pinto (joaquim.pinto@kit.edu)

**Abstract.** Extratropical cyclones are a dominant feature of the mid-latitudes, as their passage is associated with strong winds, precipitation, and temperature changes. The statistics and characteristics of extratropical cyclones over the North Atlantic region exhibit some fundamental differences between Pre-Industrial (PI) and Last Glacial Maximum (LGM) climate  
10 conditions. Here, the *statistics* are analysed based on results of a tracking algorithm applied to global PI and LGM climate simulations. During the LGM, both the number and the intensity of detected cyclones was higher compared to PI. In particular, increased cyclone track activity is detected close to the Laurentide ice sheet and over central Europe. To determine changes in cyclone *characteristics*, the top 30 extreme storm events for PI and LGM have been simulated with a regional climate model and high resolution (12.5 km grid spacing) over the eastern North Atlantic and Western Europe. Results show that LGM  
15 extreme cyclones were characterised by weaker precipitation, enhanced frontal temperature gradients, and stronger wind speeds than PI analogues. These results are in line with the view of a colder and drier Europe, characterised by little vegetation and affected by frequent dust storms, leading to reallocation and build-up of thick loess deposits in Europe.

## 1. Introduction

The day-to-day weather conditions in the mid-latitudes are strongly affected by the passage of extratropical cyclones, which  
20 **are** typically associated with precipitation, strong winds, and changes in temperature and cloudiness. Cyclones also play a major role in the water cycle and the redistribution of momentum and energy in the climate system (Hoskins and Valdez, 1990; Chang et al., 2002). The assessment of cyclone activity, notably to analyse their paths, characteristics and impacts are thus key to determine both the day-to-day weather conditions, the regional mean climate and its variability on multiple time-scales. In fact, there is a wide range of literature analysing case studies of extreme cyclones (e.g., Wernli et al., 2002; Ludwig et al.,  
25 2015), the mean cyclone activity in the mid-latitudes in the recent past (e.g., Hoskins and Hodges, 2002; Ulbrich et al., 2009) and possible changes under future climate conditions (e.g., Bengtsson et al., 2009; Ulbrich et al., 2009). On the other hand, studies analysing the structural characteristics of extratropical storms from a climatological perspective are less frequent (e.g. Catto et al., 2010; Rudeva and Gulev, 2011; Dacre et al., 2012; Hewson and Neu, 2015; Sinclair et al., 2019). While some

general concepts are available on how warmer climate conditions will affect the intensity and structure of cyclones, there are  
30 still several open questions, particularly regarding how dominant the increased latent heating may become compared to other  
physical processes like low-level and upper-level baroclinicity (see Catto et al., 2019; their Figure 2).

The availability of studies addressing the characteristics of cyclone activity outside of the period extending from the mid-19<sup>th</sup>  
Century to the end of the 21<sup>st</sup>-Century decreases sharply. Raible et al (2018) analysed variations of cyclone statistics in a very  
long simulation with a fully coupled earth system model from 850 to 2100 CE. While they identified variations on multiple  
35 time-scales, they found no evidence for an external forcing imprint before 1850. Moreover, Pfahl et al. (2015) analysed cyclone  
activity in idealised aquaplanet simulations covering a wide range of possible climate conditions (from 270K to 316K global  
mean temperatures). While the structure of the majority of the cyclones reveals only small changes on average, **larger**  
differences were identified for intense cyclones. For example, cross-front temperature differences are expected to be higher  
(lower) for considerably colder (warmer) climates (Pfahl et al., 2015, their Figure 10), whereas the associated precipitation is  
40 expected to decrease (increase; their Figure 12) due to the strong limiting effect of temperature on the atmospheric moisture  
content.

**One important issue preventing non-recent or non-21st century cyclone analysis is the availability of climate model output  
with sufficient spatial and temporal resolution to enable identification, tracking and characterisation of such cyclones.** For  
example, model data from the PMIP3 project (Braconnot et al., 2012) are only archived 6-hourly for short (30 years) time  
45 slices, and typically at a low resolution (approximately 200-300 km). Most pre-20<sup>th</sup> Century studies consider aggregated  
measures of cyclone (or synoptic) activity (e.g., Kageyama et al., 1999; Laine et al., 2009; Hofer et al., 2012; Ludwig et al,  
2016), thus not enabling a detailed comparison to regional temperature and precipitation variability. One period of particular  
interest is the Last Glacial Maximum (LGM; Clark et al., 2009), when the European climate was characterised by colder and  
mostly drier conditions (Bartlein et al., 2011; Annan and Hargreaves, 2013; Újvári et al., 2017; Cleator et al., 2019). Large  
50 parts of Northern Europe were covered by permanent ice sheets and surrounded by polar-desert conditions (Ray and Adams,  
2001). Western, Central and Eastern Europe were largely characterised by open shrublands and grasslands (steppe-tundra),  
while in Southern Europe steppe with embedded forest (forest steppe) dominated (Ray and Adams, 2001). Under these  
conditions, dust storms triggered by strong winds must have been common in Europe, as documented by the major loess  
deposits found primarily around 50°N over Western and Central Europe and over large parts of Eastern Europe (Antoine et  
55 al., 2009; 2013; Sima et al., 2013; Újvári et al., 2017).

Under the influence of the continental ice sheets and extended sea ice, the PMIP3 GCMs show **stronger** meridional temperature  
gradients, **leading to a southward displaced, more intense and less variable North Atlantic jet than under** current climate  
conditions (Löffverström et al, 2014; **2016**; Merz et al., 2015; Wang et al. 2018). These differences have been related **e.g., to**  
more dominant cyclonic Rossby wave breaking near Greenland (Riviére et al., 2010), **stationary wave packets trapped in the**  
60 **mid-latitude wave guide (Löffverström, 2020)** and to enhanced meridional eddy momentum flux convergence over the North  
Atlantic (Wang et al., 2018). **In line with a southward displaced and stronger jet stream, several studies show a more intense**



and southward shifted North Atlantic storm track compared to today's climate (e.g., Hofer et al., 2012; Luetscher et al., 2015; Ludwig et al., 2016). However, other studies display reduced storm track activity over the North Atlantic in spite of the enhanced baroclinicity (e.g. Donohoe and Battisti, 2009; Rivi re et al., 2010; L fverstr m et al., 2016). Rivi re et al. (2018) discusses a reduced baroclinic conversion as a possible reason for this apparent discrepancy, arguing that the eddy heat fluxes are less well aligned with the mean temperature gradient for LGM than for PI. Other arguments for the reduced storminess include model resolution, parameterizations and boundary conditions (e.g. Donohoe and Battisti, 2009; Rivi re et al., 2018). Thus, the intensity differences between LGM and PI North Atlantic storm track activity may be model dependent.

The PMIP3 models show indications that while Europe was largely drier than today, this is not the case for some regions, notably for Iberia (e.g., Hofer et al., 2012; Beghin et al., 2016, Ludwig et al., 2016). However, wetter conditions over Iberia are not in line with (most of) the proxy data, which themselves are often associated with considerable uncertainties (e.g., Bartlein et al., 2011; Moreno et al., 2014, Cleator et al., 2019). Nevertheless, the substantial misrepresentation of the regional climate for the LGM in PMIP3 models compared to proxies is regarded as a general issue (Harrison et al., 2015). In some cases, such caveats can be partially traced back to shortcomings of the GCMs and/or their boundary conditions. For example, Ludwig et al (2017) implemented more realistic boundary conditions in terms of the North Atlantic SSTs, land use types and vegetation cover in a regional climate model (RCM) to simulate the regional climate under LGM conditions. Their results in terms of LGM temperature, precipitation and the permafrost margin are in better agreement with the proxies than without the implemented boundary conditions. Still, further studies are needed, notably at the regional scale (e.g. Ludwig et al., 2018), in order to further our confidence in the modelling capabilities and our understanding of the paleoclimate conditions for Europe in key periods like the LGM (Harrison et al., 2015; 2016; Ludwig et al., 2019).

The present work aims to advance our understanding of the LGM climate over the North Atlantic and Europe through a more detailed analysis of the cyclonic activity and its associated impacts, notably in terms of precipitation, temperature and wind speed. The LGM cyclones are first identified and tracked on a simulation with the coupled MPI-ESM-P model, for which data with high temporal resolution was archived. Secondly, a sub-sample of extreme cyclones is downscaled with a RCM to analyse possible changes in LGM cyclone characteristics compared to their modern counterparts at high spatial and temporal resolution. The identified characteristics of LGM extreme cyclones are discussed in terms of the available proxies for LGM Climate across Western Europe. Additionally to the precipitation and temperature, the importance of the dominant land cover conditions and the frequent occurrence of dust storms is evaluated. The final section presents the summary and main conclusions.

## 2. Data and Methods

The starting point of our analysis is data from the third phase of the Paleoclimate Modeling Intercomparison Project (PMIP3) (Braconnot et al., 2012) (<http://pmip3.lscce.ipsl.fr/>). The simulations were performed according to the PMIP3 21 ka

experimental design, which includes the lower sea level and blended ice sheet data (Peltier et al., 2015, Lambeck and Chappell, 2001; Lambeck et al., 2002; Tarasov and Peltier, 2002, 2003), orbital parameters and **lower** greenhouse gas concentrations (see Table 1). From the **PMIP3** GCMs, we have selected the MPI-ESM-P (Stevens et al., 2013; Jungclaus et al., 2013) constant forcing simulations, for which two 30-year time slices with six hourly output data are available for Pre-Industrial (PI) and LGM conditions. **This choice was motivated by the availability of six hourly 3-D model level data needed for running the RCM.** Ludwig et al. (2016) recently analysed a small ensemble of PMIP3 models in terms of large-scale circulation for Europe, jet stream synoptic activity, precipitation and temperature for **the** LGM. While the MPI-ESM-P model has a **slightly different jet structure to some of the other** PMIP3 models (cf. Ludwig et al., 2016; their Figure 2), which also impacts for example the storm track and precipitation (their Figures 4, 6), its main characteristics are generally close to the ensemble average.

Individual extratropical cyclones over the North Atlantic and Europe are identified and tracked based on six hourly mean sea level pressure data with a widely used automatic tracking algorithm (Murray and Simmonds, 1991; Pinto et al. 2005). The resulting cyclone statistics provide information on the lifetime of each identified cyclone, thus enabling the computation of mean cyclone statistics like track density, mean maximum intensity, cyclogenesis, cyclolysis, propagation speed and deepening rates. Cyclone statistics obtained with this method compare well with other methodologies (e.g., Neu et al., 2013; Hewson and Neu, 2015). Following Pinto et al. (2009), cyclones are selected based on the following conditions: (a) cyclone lifetime of at least 24 h hours, (b) a minimum core MSLP value below 1000 hPa (3) a maximum vorticity (approximated by the Laplacian of MSLP) value above  $0.6 \text{ hPa deg. lat.}^{-2}$ , and (d) a maximum deepening rate of  $0.3 \text{ hPa deg. lat.}^{-2}\text{s}^{-1}$  is achieved at least once during their lifetime. The method is here applied to the MPI-ESM-P data for the extended (ONDJFM) winter season. In order to analyse the characteristics of the most extreme cyclones affecting Europe in more detail, the most intense 30 cyclones (TOP 30) for the PI and LGM periods are selected based on their peak intensity in terms of vorticity and their passage within a pre-defined box over the eastern North Atlantic (Figure 1, dashed box). The selection of the box enables the creation of a cyclone ensemble that impacts Western Europe and permits a comparison with terrestrial proxy data e.g. for precipitation and dust.

The Weather Research and Forecast (WRF) model (Skamarok et al., 2008) is used in its version 3.9.1.1 **to simulate the TOP 30 cyclones (from PI and LGM) with a grid spacing of** 12.5 km (including 35 vertical layers up to 30 hPa). To achieve a grid spacing of 12.5 km, a 2-step nesting approach is necessary. Cyclones were initially simulated on a 50 km grid forced by MPI-ESM-P data as initial and boundary conditions with an update frequency of six hours. The final 12.5 km grid spacing is achieved by a second nesting step within the WRF model. An overview of the **parameterization choices** is given in Table 2. For the calculation of wind gusts, a gust **parameterization** based on 10 m wind speed and friction velocity (Schulz and Heise, 2003; Schulz, 2008) has been implemented into the WRF model. This gust **parameterization** shows an overall good agreement with observed wind gusts, particularly over flat terrain (Born et al. 2012). For the WRF simulations, global PI and LGM boundary conditions were adapted considering specifications of the PMIP3 protocol (Braconnot et al., 2012, see also Ludwig

et al. 2017). These changes encompass orbital parameters, trace gases (see Table 1), the consideration of ice sheets (extent and height), an associated lowering of the sea level and adaption of land use cover (CLIMAP Project Members, 1984).

The TOP 30 cyclone tracks simulated by WRF were identified manually based on relative vorticity field at 850 hPa. For comparison of the PI and LGM cyclone characteristics, and following the methodology from Catto et al. (2010; their Figure 3), each track was rotated so that the cyclones were each moving in west-east direction, enabling the generation of composites for different atmospheric variables (cf. also Dacre et al., 2012). Composites have been created for peak intensity (0) and 6, 12, 18 and 24 hours before peak intensity, and 6 and 12 hours afterwards. For brevity, we will primarily discuss the time frames i) 12 hours before peak intensity and ii) peak intensity. The variables analysed from the 12.5 km WRF simulations include mean sea level pressure, precipitation, column integrated water vapour, equivalent-potential temperature 850 hPa, 925 hPa winds, near-surface wind gusts.

### 3. Northern Hemisphere Cyclone Statistics for PI and LGM conditions

In this section, we analyse the general characteristics of cyclones over the North Atlantic and Europe under LGM conditions and compare them to PI climate conditions. Figure 2 shows the cyclone track density for the extended winter for PI and LGM climate conditions. In spite of the lower spatial resolution of MPI-ESM-P, the cyclone track density for the PI is close to cyclone statistics obtained with Reanalysis datasets, with slight southerly shift of cyclonic activity (see Figure S1 for comparison with NCEP reanalysis data (Kalnay et al, 1996)), and CMIP GCMs for recent climate conditions (cp. Pinto et al., 2007; their Figure 1). Still, some regional shortcomings are identified, notably the limited cyclone activity over the Mediterranean basin. The North Atlantic storm track shows a clear tilt towards Northern Europe and the Arctic Ocean for PI, and its location and orientation are closely related with the eddy-driven jet stream (black contours in Fig. 2a) and the associated upper-air baroclinicity (Hoskins and Valdes, 1990; Pinto et al., 2009). A comparison of the jet stream between MPI-ESM-P PI and NCEP Reanalysis data shows a slight tilt towards Europe by the MPI model (Fig. S2), in line with the enhanced (reduced) southward (northward) cyclone activity (Fig. S1)

The North Atlantic storm track looks quite different under LGM conditions relative to PI: the cyclone track density is higher over the North Atlantic and more constrained to the ice edge (Fig. 2b, Fig. S1). Close to Europe, a bifurcation is found, and cyclones are either deflected northward along the border of the Scandinavian ice sheet or south-eastward towards Central Europe and the Mediterranean (Fig. 2c). In accordance, the eddy-driven jet is stronger under LGM conditions in the MPI-ESM-P (Fig. S2), thus establishing more favourable conditions for the occurrence of intense storms affecting Western and Central Europe. For the North Atlantic (70°W – 0°, 35°N – 70°N), the total number of cyclones for the analysed 30-year period is about 26% larger for LGM than for PI conditions (12071 vs. 9541 individual cyclone counts in 30 years, corresponding to roughly 2.2 cyclones/day vs 1.8 cyclones/day).

Other properties of cyclone activity are depicted in Figure 3 for LGM in terms of absolute values (left column) and their differences to PI (right column). Cyclogenesis is dominant along the North American east coast for the LGM (Fig. 3a), and much stronger than in PI (Fig. 3b), which is in line with a much stronger upper level jet stream during glacial conditions. Moreover, the rate of cyclogenesis increased south of Greenland and over Western and Central Europe. On the other hand, there is more cyclolysis along the borders of the Greenland and Scandinavian ice sheet (Fig. 3c) relative to the PI conditions (Fig. 3d). Mean maximum cyclone intensity is typically attained in a region extending from Newfoundland to Iceland and the British Isles, with a secondary maximum over Eastern Europe (Fig. 3e). Compared to the PI cyclones, the LGM cyclones have stronger intensities, particularly in an area extending from the south of Greenland to the British Isles, and over most of continental Europe. On the other hand, cyclone intensity close to the North American East coast is considerably lower (Fig. 3f). Deepening rates are stronger for LGM cyclones over the central north Atlantic, as well as their filling rates close to the ice edge / ice sheets (Fig. 3g,h). These results point towards different typical development of LGM cyclones compared to their PI counterparts, which occurs either more zonally at lower latitudes towards Central Europe or further downstream closer to the ice edge towards the Arctic.

Figure 4 displays the relative frequency distribution of the cyclone intensity over the North Atlantic area ( $70^{\circ}\text{W} - 0^{\circ}$ ,  $35^{\circ}\text{N} - 70^{\circ}\text{N}$ ), revealing that LGM cyclones are on average more intense (mean (median):  $1.58$  ( $1.41$ )  $\text{hPa deg. lat.}^{-2}\text{s}^{-1}$ ) than their PI counterparts (mean (median):  $1.43$  ( $1.28$ )  $\text{hPa deg. lat.}^{-2}\text{s}^{-1}$ ). In particular, the number of cyclones exceeding  $3 \text{ hPa deg. lat.}^{-2}\text{s}^{-1}$  is twice as large for LGM than for PI. In fact, a small number (18) of LGM cyclones attain intensities exceeding the range identified for PI cyclones. The statistics for the region close to Europe (box) are similar (not shown). All these results document a shift towards stronger intensities for LGM cyclones, both in terms of average numbers and extreme values.

#### 4. Characteristics of Extreme Cyclones over the Eastern North Atlantic

To analyse the characteristics of cyclones for the LGM, a subset of 30 extreme cyclones passing over the Eastern North Atlantic is selected for both the PI and LGM periods based on the highest values for vorticity (Laplacian of MSLP) within the selected box. The trajectories of the selected MPI-ESM cyclones are depicted in Figure 5 and key information are given in Table 3. Two important facts are clearly identifiable: LGM extreme cyclone trajectories are more zonally orientated and constrained to a narrower corridor (particularly until  $15^{\circ}\text{W}$ ) than their PI counterparts, and they achieve higher vorticity (mean Laplacian of MSLP for LGM:  $2.80$ ; PI:  $2.52$ ) values during lifetime (Tab. 3).

For each of these cyclones, WRF simulations down to  $12.5 \text{ km}$  grid-spacing are performed along the most intense segment of their lifetimes, thus gaining 3D data to analyse the cyclones e.g. in terms of the evolution of their structure, air masses, winds and precipitation. Care was taken that storms agree between the original MPI-ESM-P data and WRF cyclone tracks. Generally, the obtained tracks based on the WRF simulations reveal lower core pressures and higher vorticity than their low resolutions counterparts do. Figure 6 shows a comparison between high and low resolution data for a selected cyclone. The considered

185 cyclone tracks (MPI-ESM LGM cyclone #24) show a good superimposition for MPI-ESM, WRF 50 km and WRF 12.5 km and a good agreement of the position of maximum intensity with a slightly further south-eastward location for WRF 50 km (Fig. 6a). While the time series, centred at peak intensity, for the development of core pressure show a similar strong pressure drop for all resolutions, the relative vorticity exhibits much stronger values for the high resolution simulation (WRF 12.5 km) in comparison with the coarser realisations. Note that the WRF simulations do not cover the whole trajectory of the cyclones, and thus the time series are shorter. Figure 6c and 6d depict the corresponding precipitation patterns at peak intensity, in this case revealing more small scale structures and higher precipitation values for the 12.5 km WRF simulation.

Based on the top 30 cyclones for PI and LGM and using the composite methodology described in section 2, average cyclone characteristics are investigated for the intensification phase, focussing on the time frames (i) 12 hours before peak intensity and (ii) peak intensity. Figure 7 displays the MSLP fields for PI and LGM for peak intensity; the corresponding panels for 12 hours before peak intensity can be found in Fig. S3. The anomalies compared to the mean MSLP are displayed in colours, in order to analyse MSLP gradients (Fig. 7 a,b; S3 a,b). The core MSLP of the LGM has higher values compared to PI (LGM: 982.7 hPa, PI: 975.2 hPa). This can be explained by the lower sea levels (~120m) for LGM, causing a difference of global mean sea level pressure of about ~13 hPa (PI: 1010 hPa, LGM: 1023 hPa). Taking this into account, the LGM cyclones reach deeper MSLP values compared to the global average MSLP, being consistent with the stronger deepening rates for LGM cyclones identified by the tracking algorithm (Fig.3 g,h). Additionally, the closer isobars south of the cyclone core indicate stronger pressure gradients for the LGM cyclones, which is supported by the LGM – PI differences (Fig. 7c). This is particularly the case on the expected location of the frontal areas. Fig. 7 (d,e) and Fig. S3 (d,e) displays the anomalies of potential temperature at 850 hPa for LGM relative to PI. Results show that the cross-frontal gradients are particularly intense across the warm front and that the whole development is displaced forward in the cyclone for LGM conditions, indicating a faster occlusion (Fig. 7 f). On the other hand, the total water content is much higher under PI conditions, primarily due to the effect of the higher environmental temperatures (Fig. 7 g,h; Fig. S3 g,h) with differences in the warm sector reaching up to 10 mm and 6-8 mm close to the cyclone core at peak intensity (Fig. 7i).

The strong difference in available water content again leads to a large difference in terms of accumulated precipitation, which is clearly larger for the PI composites (Fig. 8 a,b; Fig. S4 a,b). While some of the smaller deviations can be potentially attributed to slightly different developments, the total precipitation is considerably lower for the LGM extreme cyclones (up to 1.7 mm h<sup>-1</sup>) particularly in the area of peak precipitation close to the cyclone centre (Fig. 8c). On the other hand, wind speed at 925 hPa is much higher for LGM cyclones (Fig. 8 d,e; Fig. S4 d,e), where wind speeds over large areas south of the cyclone exceed their PI counterparts by 10-12 ms<sup>-1</sup>, particularly for 12 hours before peak intensity (Fig. 8 f; Fig. S4 f). Strong differences are also revealed for near-surface wind gusts (Fig. 8 g-i; Fig. S4 g-i). In this case, the wind gusts are particularly enhanced along the expected location of the cold front at peak intensity, with deviations exceeding 5 ms<sup>-1</sup>. The above described patterns remain true for the cyclone characteristics 12 hours after peak intensity (Figs S5, S6). For example, stronger wind gusts remain dominant in the area south of the cyclone core (Fig. S4i).

In summary, LGM cyclones display steeper MSLP gradients (in agreement with higher intensity in terms of circulation), larger temperature gradients between the air masses, weaker precipitation and stronger wind gusts than their PI counterparts do (see also summary for wind and precipitation in Table S1).

## 5. Discussion with available proxy-based climate reconstructions

The above analysis shows that extreme cyclones under LGM conditions were typically more intense than PI extreme cyclones. Likewise, they were associated with larger frontal temperature gradients, stronger winds and reduced precipitation. In this section, we analyse in how far these cyclone characteristics can help to explain the climate conditions in Western and Central Europe at the LGM and the frequent occurrence of dust storms in that area.

According to the available proxy records, Western and Central Europe were colder and largely drier under LGM conditions (Bartlein et al., 2011; Annan and Hargreaves, 2013; Cleator et al., 2019), and was to a large extent covered by open shrublands and grasslands (Ray and Adams, 2001). The colder and generally drier conditions are reproduced by the PMIP3 GCMs, but considerable differences in detail have been identified compared to proxy-based climate reconstructions (Beghin et al., 2016; Ludwig et al., 2016; Cleator et al., 2019). These can be both attributed to shortcomings of the GCMs and/or uncertainties in the reconstructions, which are often not well constrained (Bartlein et al., 2011; Ludwig et al., 2019; Cleator et al., 2019). For example, most PMIP3 GCMs show enhanced precipitation over the Iberian Peninsula compared to PI climate (Beghin et al., 2016; Ludwig et al., 2016), which disagrees with the proxy data (e.g. Bartlein et al., 2011). Later, Ludwig et al (2017, 2018) show that the wet bias over Iberia and Western Europe can strongly be reduced by considering more realistic boundary conditions (particularly in terms of sea surface temperatures, land use and vegetation cover) in high-resolution RCM simulations.

The present results enable a more detailed evaluation of the above hypotheses and interpretations. Under current climate conditions, precipitation in the mid-latitudes is largely associated with the passage of extratropical cyclones, where extreme cyclones have a comparatively larger contribution to total/extreme precipitation (Pfahl and Wernli, 2012; Hawcroft et al. 2012). Hawcroft et al. (2016) have provided evidence that GCMs typically have shortcomings in representing the precipitation associated with mid-latitude cyclones. It is reasonable to assume that those shortcomings may be exacerbated at lower resolutions, e.g. those typical of the PMIP3 models. An idealised study by Pfahl et al. (2015) has shown that precipitation increases (decreases) disproportionately in considerably warmer (colder) climate conditions. With the help of the high resolution WRF simulations, we could provide evidence that extreme cyclones under LGM conditions indeed induce considerably less precipitation than their PI counterparts (~22% within a 10° radius around the cyclone centre). Even though lower cyclone-related precipitation may be partially compensated by enhanced moisture advection embedded in the (stronger) westerly large-scale flow, particularly for areas where orographic precipitation dominates (e.g. upward slopes of mountain ranges / glaciers), it is consistent with the hypothesis of a drier Western and Central Europe. The view of a drier Europe is also

consistent with the dominant land cover types estimated from proxy data (Ray and Adams, 2001) or a statistical reconstruction based on temperature and precipitation (Shao et al., 2018), namely polar desert close to the glaciers, forest steppe over Southern Europe and steppe in-between. The fact that we have selected an area close to the Iberian Peninsula for cyclone selection leads to the strong assumption that largely drier conditions must also have been found for Southwestern Europe, in agreement with the proxies (e.g. Bartlein et al., 2011, Moreno et al., 2014).

Mineral dust plays an important role in our climate system (Shao et al., 2011). Dust emissions are typically initiated by the wind stress on land surfaces with little to no vegetation cover and easily erodible soils (e.g., Prospero et al., 2002). Such areas were very common in Europe under LGM conditions (e.g., Ray and Adams, 2001, Ugan and Byers, 2007), when the global dust cycle is estimated to have been stronger than at present (Maher et al., 2010). A large number of loess deposits over Western and Central Europe (particularly around 50°N; Antoine et al., 2009) indicate that dust storms were a common feature of the European climate. In particular, Antoine et al. (2009) identified cyclic variations in loess deposition between 34-17 ka on several sites in France, Germany and Belgium, with particularly high sedimentation rates, and attributed these to numerous and intense dust storms in periods with stronger large-scale flow and reduced precipitation. Furthermore, the high accumulation rates of loess in the middle and lower Danube basin indicate cold, dry and windy conditions during the LGM in south-eastern Europe (Fitzsimmons et al, 2012), consistent with increased storm activity over Central Europe (Fig. 2c). These and other findings document a more intense (global) dust cycle for LGM conditions (e.g. Albani et al., 2016; Újvári et al., 2017; Albani and Mahowald, 2019). The occurrence of dust storms over Western and Central Europe has been conceptually associated with the passage of intense extratropical cyclones penetrating deep into the continent (Antoine et al., 2009; their Figure 12). Following on previous studies (e.g. Laine et al., 2009; Hofer et al. 2012; Ludwig et al., 2016), the present results provide evidence for the first time that individual LGM cyclones would be indeed capable of triggering such dust events: their frequent tracks over Western/Central Europe and strong wind could easily trigger dust emission and transport over short (for coarse grain) and large (for fine grain material) distances (cp. Shao et al. 2011). As moisture acts to make surface dust particles more cohesive (e.g., Ishizuka et al., 2008), the reduced cyclone precipitation and higher wind speeds in LGM cyclones would have actually been more conducive to generating dust storms. In addition to the role of the westerlies and embedded cyclones into generating dust storms in Europe, there is evidence that situations with persistent easterlies associated with anticyclonic flow triggered by a strong anticyclone over the Scandinavian ice sheet may have also played a significant role for loess deposition not only over Eastern Europe but also over Central Europe (Újvári et al., 2017; Schaffernicht et al., 2019).

## 6. Summary and Conclusions

The statistics and characteristics of extratropical cyclones over the North Atlantic and Western Europe were analysed for time-slice experiments for PI and LGM conditions. First, the statistics of the climatologies of PI and LGM cyclones are analysed and compared based on global MPI-ESM-P simulations. Second, the characteristics of extreme LGM cyclones over the Eastern



280 North Atlantic were analysed in detail based on high-resolution simulations (12.5 km grid-spacing) with the RCM WRF and compared to their PI counterparts. The results were discussed with available proxy reconstructions of climate parameters and vegetation types. The main conclusions are as follows:

- The North Atlantic storm track was more intense under LGM conditions, featuring more frequent and intense synoptic systems than under PI conditions. One of the downstream branches brought more often extreme cyclones towards Western and Central Europe and the Mediterranean area.
- LGM cyclones were more intense due to stronger baroclinicity with less influence from diabatic processes (lower rainfall and lower water vapour content). In particular, LGM cyclones benefit from a stronger and extended jet stream. The development was typically faster, with deepening rates and peak intensities exceeding those from PI cyclones.
- LGM extreme cyclones were characterised by lower precipitation, enhanced frontal temperature gradients, and stronger mean wind speeds and wind gusts than PI analogues.
- These characteristics are in line with the view of a colder and drier Europe, characterised by steppe/tundra land types and affected by frequent dust storms, leading to reallocation and build-up of thick loess deposits.

Given that this study is based on a single GCM, a single tracking method and a single RCM, it should be regarded as a preliminary analysis as the uncertainties of the jet stream position and storm track activity (e.g., Merz et al, 2013, Riviere et al., 2018) may be considerable among different GCMs. Still, the identified differences between PI and LGM (extreme) cyclones are unequivocal, are consistent with idealised studies, demonstrate the potential of the approach and may become instrumental to facilitate a better interpretation of LGM proxy data. In particular, this study provides new understanding of the relationship between the large scale mean cyclone activity and short term variability on the regional scale and thus may help to reduce numerical interpretative uncertainties (Harrison et al. 2016).

Even though the added value of RCMs in paleoclimate applications is still controversially discussed (Armstrong et al., 2019), there is a general call for improvements towards a new generation of reliable regional projections (e.g., Harrison et al., 2015; Kageyama et al., 2018). The present and other studies (see Ludwig et al., 2019 for a review) provide clear arguments for the extended use of RCMs in the scope of paleoclimate studies, as they can play an important role towards a meaningful joint interpretation of proxies and climate model data. The upcoming new paleoclimate simulations within CMIP6/PMIP4 (Kageyama et al., 2017, 2018), as well as new proxy-based reconstructions of climates (Cleator et al. 2019), will provide novel possibilities to expand our understanding of past climates and to reduce uncertainties on both the numerical and reconstruction branches.

**Data availability:** WRF-Data presented in the paper can be accessed by contacting the authors. The data will be archived at the DKRZ (German Climate Computing Centre). PMIP3 boundary conditions can be obtained at <https://pmip3.lsce.ipsl.fr/>

310 (last access: 12 November 2019). Vegetation cover and Landuse data from CLIMAP can be obtained at <https://iridl.ldeo.columbia.edu/SOURCES/.CLIMAP/.LGM/> (last access: 12 November 2019).

**Author contributions:** Both authors contributed equally to this work. JGP and PL designed the study and the experiments. PL developed the paleo-specific model adjustments, performed the simulations and prepared the figures. JGP wrote the first draft of the manuscript. JGP and PL contributed with revisions.

315 **Competing interests:** The authors declare that they have no conflict of interest.

**Acknowledgements:** We thank the German Climate Computing Centre (DKRZ, Hamburg) for providing the MPI-ESM-P data and computing resources within DKRZ Project 965 “Our Way to Europe – Palaeoclimate and Palaeoenvironmental reconstructions”. JGP thanks the AXA Research Fund for support, and both authors thank REKLIM (Helmholtz Climate Initiative regional climate change) for partial funding. Thanks to Alexander Reinbold for his contribution to a preliminary analysis, and Sven Ulbrich for help with the cyclone statistics. The authors also thank the PALEOLINK project by the PAGES 2kNetwork coordinators. We acknowledge support by Deutsche Forschungsgemeinschaft (DFG) and Open Access Publishing Fund of Karlsruhe Institute of Technology. **We thank two anonymous reviewers and M. Löffverström for the detailed and helpful comments.**

**References**

325 Albani, S., Mahowald, N.M., Murphy, L.N., Raiswell, R., Moore, J.K., Anderson, R. F., McGee, D., Bradtmiller, L.I., Delmonte, B., Hesse, P. P., et al.: Paleodust variability since the Last Glacial Maximum and implications for iron inputs to the ocean, *Geophys. Res. Lett.*, 43, 3944–3954, doi:10.1002/2016GL067911, 2016.

Albani, S. and Mahowald, N.M.: Paleodust Insights into Dust Impacts on Climate. *J. Climate*, 32, 7897–7913, doi:10.1175/JCLI-D-18-0742.1, 2019.

330 Annan, J. D., and Hargreaves, J. C.: A new global reconstruction of temperature changes at the Last Glacial Maximum, *Clim. Past*, 9, 367–376, doi:10.5194/cp-9-367-2013, 2013.

Antoine, P., Rousseau, D.-D., Moine, O., Kunesch, S., Hatté, C., Lang, A., Tissoux, H., and Zöller, L.: Rapid and cyclic aeolian deposition during the Last Glacial in European loess: a high-resolution record from Nussloch, Germany, *Quat. Sci. Rev.*, 28, 2955–2973, doi:10.1016/j.quascirev.2009.08.001, 2009.

335 Antoine, P., Rousseau, D. D., Degeai, J.-P., Moine, O., Lagroix, F., Kreutzer, S., Fuchs, M., Hatté, C., Gauthier, C., Svoboda, J., and Lisa, L.: High-resolution record of the environmental response to climatic variations during the Last Interglacial-

- Glacial cycle in Central Europe: the loess-paleosol sequence of Dolni Vestonice (Czech Republic), *Quaternary Sci. Rev.*, 67, 17–38, doi:10.1016/j.quascirev.2013.01.014, 2013.
- Armstrong, E., Hopcroft, P. O., and Valdes, P.: Reassessing the value of regional climate modelling using palaeoclimate  
340 simulations. *Geophysical Research Letters*, 46, doi:10.1029/2019GL085127, 2019.
- Bartlein, P. J., et al.: Pollen-based continental climate reconstructions at 6 and 21 ka: A global synthesis, *Clim. Dyn.*, 37, 775–  
802, doi:10.1007/s00382-010-0904-1, 2011.
- Beghin, P., Charbit, S., Kageyama, M., Combourieu-Nebout, N., Hatté, C., Dumas, C., Peterschmitt, J.-Y.: What drives LGM  
precipitation over the western Mediterranean? A study focused on the Iberian Peninsula and northern Morocco, *Clim.*  
345 *Dyn.*, 46, 2611– 2631, doi:10.1007/s00382-015-2720-0, 2016.
- Bengtsson L., Hodges K.I., and Keenlyside N.: Will extratropical storms intensify in a warmer climate? *J. Clim.* 22: 2276–  
2301, doi:10.1175/2008JCLI2678.1, 2009.
- Born K., Ludwig P., Pinto J.G.: Wind gust estimation for Mid-European winter storms: Towards a probabilistic view. *Tellus*  
A, 64, 17471, doi:10.3402/tellusa.v64i0.17471, 2012.
- 350 Braconnot, P., Harrison, S. P., Kageyama, M., Bartlein, P. J., Masson-Delmotte, V., Abe-Ouchi, A., Otto-Bliesner, B., and  
Zhao, Y.: Evaluation of climate models using palaeoclimatic data, *Nat. Clim. Change*, 2, 417– 424,  
doi:10.1038/nclimate1456, 2012.
- Catto, J.L., Ackerley, D., Booth, J., Champion, A., Colle, B., Pfahl, S., Pinto, J.G., Quinting, J., and Seiler, C.: The Future of  
Extratropical Cyclones. *Curr Clim Change Rep*, doi:10.1007/s40641-019-00149-4, 2019.
- 355 Catto, J. L., Shaffrey, L. C., and Hodges, K. I.: Can climate models capture the structure of extratropical cyclones?, *J. Clim.*,  
23, 1621– 1635. doi:10.1175/2009JCLI3318.1, 2010.
- Chang, E.K. M., Lee, S., and Swanson, K.L.: Storm track dynamics. *J. Clim.*, 15, 2163–2183, doi: 10.1175/1520-  
0442(2002)015<02163:STD>2.0.CO;2, 2002.
- Clark, P.U., et al.: The Last Glacial Maximum. *Science* 325, 710–714. doi:10.1126/science.1172873, 2009.
- 360 Cleator, S.F., Harrison, S.P., Nichols, N.K., Prentice, I.C., and Roulstone, I.: A new multi-variable benchmark for Last Glacial  
Maximum climate simulations, *Clim. Past Discuss.*, doi:10.5194/cp-2019-55, 2019.
- CLIMAP Project Members: The last interglacial ocean, *Quat. Res.*, 2, 123–224, doi:10.1016/0033-5894(84)90098-X, 1984.
- Dacre, H.F., Hawcroft, M.K., Stringer, M.A., and Hodges, K.I.: An extratropical cyclone database: A tool for illustrating  
cyclone structure and evolution characteristics, *Bull. Amer. Met. Soc.*, doi: 10.1175/BAMS-D-11-00164.1, 2012.
- 365 Donohoe, A., and Battisti, D.S.: Causes of Reduced North Atlantic Storm Activity in a CAM3 Simulation of the Last Glacial  
Maximum. *J. Climate*, 22, 4793–4808, doi:10.1175/2009JCLI2776.1, 2009.
- Ferrier, B. S., Tao, W.-K., and Simpson, J.: A double-moment multiple-phase four-class bulk ice scheme. Part II: Simulations  
of convective storms in different large-scale environments and comparisons with other bulk parameterizations, *Journal*  
*of the atmospheric sciences*, 52, 8, 1001-1033, doi: 10.1175/1520-0469(1995)052<1001:ADMMPF>2.0.CO;2, 1995.

- 370 Fitzsimmons, K.E., Markovic, S. B., and Hambach, U.: Pleistocene environmental dynamics recorded in the loess of the middle and lower Danube basin, *Quaternary Science Reviews*, 41, 104–118, doi:10.1016/j.quascirev.2012.03.002, 2012.
- Hawcroft, M.K., Shaffrey, L.C., Hodges, K.I., and Dacre, H.F.: How much Northern Hemisphere precipitation is associated with extratropical cyclones?, *Geophys. Res. Lett.*, 39, L24809, doi:10.1029/2012GL053866, 2012.
- Hawcroft, M.K., Shaffrey, L.C., Hodges, K.I., and Dacre, H.F.: Can climate models represent the precipitation associated with extratropical cyclones?, *Clim. Dyn.*, 47: 679–695, doi:10.1007/s00382-015-2863-z, 2016.
- 375 Harrison, S.P., Bartlein, P.J., Izumi, K., Li, G., Annan, J., Hargreaves, J., Braconnot, P., and Kageyama, M.: Evaluation of CMIP5 palaeo-simulations to improve climate projections, *Nat. Clim. Chang.*, 5, 735–743, doi:10.1038/nclimate2649, 2015.
- Harrison, S.P., Bartlein, P. J., and Prentice, I.C.: What have we learnt from palaeoclimate simulations?, *J. Quat. Sci.*, 31, 363–385, doi:10.1002/jqs.2842, 2016.
- 380 Hewson, T. D., and Neu U.: Cyclones, windstorms and the IMILAST project, *Tellus A*, 67, 27128, doi:10.3402/tellusa.v67.27128, 2015.
- Hofer, D., Raible, C.C., Dehnert, A., and Kuhleemann, J.: The impact of different glacial boundary conditions on atmospheric dynamics and precipitation in the North Atlantic region, *Clim. Past*, 8, 935– 949, doi:10.5194/cp-8-935-2012, 2012.
- 385 Hoskins B.J., and Hodges K.I.: New perspectives on the Northern Hemisphere winter storm tracks. *J. Atmos. Sci.* 59: 1041 – 1061, doi:10.1175/1520-0469(2002)059<1041:NPOTNH>2.0.CO;2, 1990.
- Hoskins, B.J., and Valdes, P. J.: On the existence of storm tracks, *J. Atmos. Sci.*, 47, 1854– 1864. doi:10.1175/1520-0469(1990)047<1854:OTEOST>2.0.CO;2, 1990.
- Iacono, M.J., Delamere, J.S., Mlawer, E.J., Shephard, M.W., Clough, S.A., and Collins W.D.: Radiative forcing by long-lived greenhouse gases: Calculations with the AER radiative transfer models. *J. Geophys. Res.*, 113, D13103. doi:10.1029/2008JD009944, 2008
- 390 Ishizuka, M., Mikami, M., Leys, J., Yamada, Y., Heidenreich, S., Shao, Y., and McTainsh, G. H.: Effects of soil moisture and dried raindroplet crust on saltation and dust emission, *J. Geophys. Res.*, 113, D24212, doi:10.1029/2008JD009955, 2008.
- 395 Janjić, Z.I.: The Step-Mountain Eta Coordinate Model: Further Developments of the Convection, Viscous Sublayer, and Turbulence Closure Schemes. *Mon. Wea. Rev.*, 122, 927–945, doi:10.1175/1520-0493(1994)122<0927:TSMECM>2.0.CO;2, 1994.
- Jungclaus, J. H., Fischer, N., Haak, H., Lohmann, K., Marotzke, J., Matei, D., Mikolajewicz, U., Notz, D., and von Storch, J.-S.: Characteristics of the ocean simulations in the Max Planck Institute Ocean Model (MPIOM) the ocean component of the MPI-Earth system model. *J. Adv. Model. Earth Syst.*, 5, 422–446, doi: 10.1002/jame.20023, 2013.
- 400 Kageyama, M., Valdes, P. J., Ramstein, G., Hewitt, C., and Wyputta, U.: Northern Hemisphere storm tracks in present day and Last Glacial Maximum climate simulations: A comparison of the European PMIP models, *J. Clim.*, 12, 742– 760, doi:10.1175/1520-0442(1999)012<0742:NHSTIP>2.0.CO;2, 1999.

- Kageyama, M., et al.: The PMIP4 contribution to CMIP6 – Part 4: Scientific objectives and experimental design of the PMIP4-  
 405 CMIP6 Last Glacial Maximum experiments and PMIP4 sensitivity experiments. *Geosci. Model Dev.*, 10, 4035–4055,  
 doi:10.5194/gmd-10-4035-2017, 2017.
- Kageyama, M., et al.: The PMIP4 contribution to CMIP6 – Part 1: Overview and overarching analysis plan. *Geosci. Model  
 Dev.*, 11, 1033–1057, doi: 10.5194/gmd-11-1033-2018, 2018.
- Kalnay, E., M. et al.: The NCEP/NCAR 40-Year Reanalysis Project. *Bull. Amer. Meteor. Soc.*, 77, 437–472,  
 410 doi:10.1175/1520-0477(1996)077<0437:TNYRP>2.0.CO;2, 1996.
- Laîné, A., Kageyama, M., Salas-Mélia, D., Voldoire, A., Rivière, G., Ramstein, G., Planton, S., Tyteca, S., and Peterschmitt,  
 J.Y.: Northern Hemisphere storm tracks during the Last Glacial Maximum in the PMIP2 ocean-atmosphere coupled  
 models: Energetic study, seasonal cycle, precipitation, *Clim. Dyn.*, 32, 593-614, doi:10.1007/s00382-008-0391-9, 2009.
- Lambeck, K., and Chappell, J.: Sea level change through the last glacial cycle, *Science*, 292, 679– 686,  
 415 doi:10.1126/science.1059549, 2001.
- Lambeck, K., Yokoyama, Y., and Purcell, A.: Into and out of the Last glacial Maximum sea level change during Oxygen  
 Isotope Stages 3–2, *Quat. Sci. Rev.*, 21, 343– 360, doi:10.1016/S0277-3791(01)00071-3, 2002.
- Löfverström, M., Caballero, R., Nilsson, J., and Kleman, J.: Evolution of the large-scale atmospheric circulation in response  
 to changing ice sheets over the last glacial cycle, *Clim. Past*, 10, 1453-1471, doi:10.5194/cp-10-1453-2014, 2014.
- 420 Löfverström, M., Caballero, R., Nilsson, J., and Messori, G.: Stationary wave reflection as a mechanism for zonalising Atlantic  
 winter jet at the LGM, *J. Atmos. Sci.*, 73, 3329– 3342, doi:10.1175/JAS-D-15-0295.1, 2016.
- Löfverström, M.: A dynamic link between high-intensity precipitation events in southwestern North America and Europe at  
 the Last Glacial Maximum, *Earth Planet. Sci. Lett.*, 534, 116081, doi:10.1016/j.epsl.2020.116081, 2020
- Luetscher, M., Boch, R., Sodemann, H., Spötl, C., Cheng, H., Edwards, R.L., Frisia, S., Hof, F., and Muller, W.: North  
 425 Atlantic storm track changes during the Last Glacial Maximum recorded by Alpine speleothems, *Nat. Commun.*, 6,  
 6344, doi:10.1038/ncomms7344, 2015.
- Ludwig, P., Pinto, J.G., Hoepp, S.A., Fink, A.H., and Gray, S.L.: Secondary cyclogenesis along an occluded front leading to  
 damaging wind gusts: windstorm Kyrill, January 2007. *Mon Weather Rev*, 143, 1417–1437. doi:10.1175/MWR-D-14-  
 00304.1, 2015.
- 430 Ludwig, P., Schaffernicht, E.J., Shao, Y., and Pinto, J.G.: Regional atmospheric circulation over Europe during the Last Glacial  
 Maximum and its links to precipitation, *J. Geophys. Res. Atmos.*, 121, 2130-2145, doi:10.1002/2015JD024444, 2016.
- Ludwig, P., Pinto, J.G., Raible, C.C., and Shao, Y.: Impacts of surface boundary conditions on regional climate model  
 simulations of European climate during the Last Glacial Maximum, *Geophys. Res. Lett.*, 44, 5086– 5095,  
 doi:10.1002/2017GL073622, 2017.
- 435 Ludwig, P., Shao, Y., Kehl, M., Weniger, G.-C.: The Last Glacial Maximum and Heinrich event I on the Iberian Peninsula: A  
 regional climate modelling study for understanding human settlement patterns. *Global and planetary change*, 170, 34–  
 47. doi:10.1016/j.gloplacha.2018.08.006, 2018.

- Ludwig, P., Gómez-Navarro, J.J., Pinto, J.G., Raible, C.C., Wagner, S. and Zorita, E.: Perspectives of regional paleoclimate modeling. *Ann. N.Y. Acad. Sci.*, 1436: 54-69. doi:10.1111/nyas.13865, 2019.
- 440 Maher, B.A., Prospero, J.M., Mackie, D., Gaiero, D., Hesse, P.P., and Balkanski, Y.: Global connections between aeolian dust, climate and ocean biogeochemistry at the present day and at the last glacial maximum, *Earth-Science Reviews*, 99, 61–97, doi:10.1016/j.earscirev.2009.12.001, 2010.
- Merz, N., Raible, C.C., and Woollings, T.: North Atlantic eddy-driven jet in interglacial and glacial winter climates, *J. Clim.*, 28, 3977-3997, doi:10.1175/JCLI-D-14-00525, 2015.
- 445 Moreno, A., Svensson, A., Brooks, S.J., Connor, S., Engels, S., Fletcher, W., Genty, D., Heiri, O., Labuhn, I., Perşoiu, A., Peyron, O., Sadori, L., Valero-Garcés, B., Wulf, S., and Zanchetta, G.: A compilation of western European terrestrial records 60-8kaBP: towards an understanding of latitudinal climatic gradients. *Quat. Sci. Rev.* 106, 167–185. doi:10.1016/j.quascirev.2014.06.030, 2014.
- Murray, R.J., and Simmonds, I.: A numerical scheme for tracking cyclone centres from digital data. Part I: Development and  
450 operation of the scheme, *Aust. Meteorol. Mag.*, 39, 155– 166, 1991.
- Neu, U., et al.: IMILAST: A community effort to intercompare extratropical cyclone detection and tracking algorithms, *Bull. Am. Meteorol. Soc.*, 94, 529– 547. doi:10.1175/BAMS-D-11-00154.1, 2013.
- Peltier, W.R., Argus, D.F., and Drummond, R.: Space geodesy constrains ice age terminal deglaciation: The global ICE-6G\_C (VM5a) model, *J. Geophys. Res. Solid Earth*, 119, 450-487, doi:10.1002/2014JB011176, 2015.
- 455 Pfahl, S., and Wernli, H.: Quantifying the Relevance of Cyclones for Precipitation Extremes. *J. Climate*, 25, 6770–6780, doi:10.1175/JCLI-D-11-00705.1, 2012.
- Pfahl, S., O’Gorman, P., and Singh, M.S.: Extratropical cyclones in idealized simulations of changed climates, *J. Clim.*, 28, 9373-9392, doi:10.1175/JCLI-D-14-00816.1, 2015.
- Pinto, J.G., Ulbrich, U., Leckebusch, G.C., Spanghel, T., Reyers, M., Zacharias, S.: Changes in storm track and cyclone activity  
460 in three SRES ensemble experiments with the ECHAM5/MPI-OM1 GCM. *Clim Dyn* 29, 195–210. doi:10.1007/s00382-007-0230-4, 2007.
- Pinto, J.G., Zacharias, S., Fink, A.H., Leckebusch, G.C., and Ulbrich, U.: Factors contributing to the development of extreme North Atlantic cyclones and their relationship with the NAO, *Clim. Dyn.*, 32, 711-737. doi:10.1007/s00382-008-0396-4, 2009.
- 465 Prospero, J.M., Ginoux, P., Torres, O., Nicholson, S.E., and Gill, T.E.: Environmental characterization of global sources of atmospheric soil dust identified with the Nimbus 7 Total Ozone Mapping Spectrometer (TOMS) Absorbing Aerosol Product, *Rev. Geophys.*, 40, 1002, doi:10.1029/2000RG000095, 2002.
- Raible, C.C., Messmer, M., Lehner, F., Stocker, T.F., Blender, R.: Extratropical cyclone statistics during the last millennium and the 21st century. *Clim. Past*, 14, 1499-1514, doi: 10.5194/cp-14-1499-2018., 2018.
- 470 Ray, N., Adams, J.M.: A GIS-based Vegetation Map of the World at the Last Glacial Maximum (25,000–15,000 BP). *Internet Archaeology*, 11. doi:10.11141/ia.11.2, 2001.

- Rivière, G., Lainé, A., Lapeyre, G., Salas-Mélia, D., and Kageyama, M.: Links between Rossby wave breaking and the North Atlantic Oscillation–Arctic Oscillation in present day and Last Glacial Maximum climate simulations. *J Clim*, 23, 2987–3008, doi:10.1175/2010JCLI3372.1, 2010.
- 475 Rivière, G., Berthou, S., Lapeyre, G., and Kageyama, M.: On the Reduced North Atlantic Storminess during the Last Glacial Period: The Role of Topography in Shaping Synoptic Eddies. *J. Climate*, 31, 1637–1652, doi:10.1175/JCLI-D-17-0247.1, 2018
- Rudeva, I., Gulev S.K.: Composite Analysis of North Atlantic Extratropical Cyclones in NCEP–NCAR Reanalysis Data. *Mon Wea Rev*, 139, 1419–1446, doi:10.1175/2010MWR3294.1, 2011.
- 480 Schaffernicht, E.J., Ludwig, P., and Shao, Y.: Linkage between Dust Cycle and Loess of the Last Glacial Maximum in Europe. *Atmos. Chem. Phys. Discuss.*, doi:10.5194/acp-2019-693, 2019.
- Schulz, J.-P.: Revision of the turbulent gust diagnostics in the COSMO model. *COSMO Newsletter* 8, 17-22. Online at: [www.cosmo-model.org](http://www.cosmo-model.org), 2008.
- Schulz, J.-P., and Heise, E.: A new scheme for diagnosing near-surface convective gusts. *COSMO Newsletter* 3, 221-225. Online at: [www.cosmo-model.org](http://www.cosmo-model.org), 2003.
- 485 Sinclair, V. A., Rantanen, M., Haapanala, P., Räisänen, J., and Järvinen, H.: The characteristics and structure of extra-tropical cyclones in a warmer climate, *Weather Clim. Dynam. Discuss.*, doi:10.5194/wcd-2019-2, 2019.
- Skamarock, W.C., Klemp, J. B., Dudhia, J., Gill, D.O., Barker, D.M., Duda, M.G., Huang, X.-Y., Wang, W., and Powers, J. G.: A description of the advanced research WRF version 3, NCAR Tech. Note NCAR/TN-475+STR, 113 pp., doi:10.5065/D68S4MVH, 2008.
- 490 Shao, Y., Anhäuser, A., Ludwig, P., Schlüter, P., and Williams, E.: Statistical reconstruction of global vegetation for the last glacial maximum, *Global Planet Change*, 168, 67-77, doi:10.1016/j.gloplacha.2018.06.002, 2018.
- Shao, Y., Wyrwoll, K.-H., Chappell, A., Huang, J., Lin, Z., McTainsh, G.H., Mikami, M., Tanaka, T.Y., Wang, X., and Yoon, S.: Dust cycle: An emerging core theme in Earth system science, *Aeol. Res.*, 2, 181-204, 2011.
- 495 Stevens, B., et al.: Atmospheric component of the MPI-M Earth system model: ECHAM6, *J. Adv. Model. Earth Syst.*, 5, 146-172, doi:10.1002/jame.20015, 2013.
- Tarasov, L., and Peltier, W. R.: Greenland glacial history and local geodynamic consequences, *Geophys. J. Int.*, 150, 198-229, doi:10.1046/j.1365-246X.2002.01702.x, 2002.
- Tarasov, L., and Peltier, W.R.: Greenland glacial history, borehole constraints, and Eemian extent, *J. Geophys. Res.*, 108, 2143, doi:10.1029/2001JB001731, 2003.
- 500 Tewari, M., Chen, F., Wang, W., Dudhia, J., LeMone, M.A., Mitchell, K., Ek, M., Gayno, G., Wegiel J., and Cuenca, R.H.: Implementation and verification of the unified NOAH land surface model in the WRF model, 20th conference on weather analysis and forecasting/16th conference on numerical weather prediction, pp. 11–15, 2004
- Ugan, A., and Byers, D.: Geographic and temporal trends in proboscidean and human radiocarbon histories during the late Pleistocene, *Quaternary Science Reviews*, 26, 3058–3080, doi:10.1016/j.quascirev.2007.06.024, 2007.
- 505



- Újvári, G., Stevens, T., Molnár, M., Demény, A., Lambert, F., Varga, G., Jull, AJT., Páll-Gergely, B., Buylaert, J.P., and Kovács, J.: Coupled European and Greenland last glacial dust activity driven by North Atlantic climate. *Proc Natl Acad Sci USA*, 114, E10632-E10638, doi:10.1073/pnas.1712651114, 2017
- 510 Ulbrich, U., Leckebusch, G. C., and Pinto, J. G.: Extra-tropical cyclones in the present and future climate: A review, *Theor. Appl. Climatol.*, 96, 117-131. doi:10.1007/s00704-008-0083-8, 2009.
- Wang, N., Jiang, D., and Lang, X.: Northern Westerlies during the Last Glacial Maximum: results from CMIP5 simulations. *J. Clim.* 31, 1135-1153. Doi: 10.1175/JCLI-D-17-0314.1, 2018.
- Wernli H., Dirren S., Liniger M.A., and Zillig M.: Dynamical aspects of the life cycle of the winter storm ‘Lothar’ (24–26 December 1999). *Q. J. R. Meteorol. Soc.*, 128, 405– 429. doi:10.1256/003590002321042036, 2002.
- 515 Zhang, C., Wang, Y., and Hamilton, K.: Improved Representation of Boundary Layer Clouds over the Southeast Pacific in ARW-WRF Using a Modified Tiedtke Cumulus Parameterization Scheme. *Mon. Wea. Rev.*, 139, 3489–3513, doi:10.1175/MWR-D-10-05091.1, 2011.

520

**Table 1.** Boundary conditions adapted in the WRF simulations for PI and LGM based on the PMIP3 protocol.

|     | CO <sub>2</sub> | N <sub>2</sub> O | CH <sub>4</sub> | Eccentricity | Obliquity | Angular<br>Precession |
|-----|-----------------|------------------|-----------------|--------------|-----------|-----------------------|
| PI  | 280 ppm         | 270 ppb          | 760 ppb         | 0.01672      | 23.446 °  | 102.04                |
| LGM | 185 ppm         | 200 ppb          | 350 ppb         | 0.01899      | 22.949 °  | 114.42                |

**Table 2.** Physical parametrization schemes used in the regional model simulations (same parametrizations used for 50 km and 12.5 km domain).

|                        | microphysics              | cumulus<br>scheme      | PBL-scheme                          | Radiation<br>scheme        | surface                 |
|------------------------|---------------------------|------------------------|-------------------------------------|----------------------------|-------------------------|
| WRF-namelist<br>option | <b>95</b> (Eta (Ferrier)) | <b>6</b> (Tiedke)      | <b>2</b> (Mellor–<br>Yamada–Janjic) | SW/LW: <b>4</b><br>(RRTMG) | <b>2</b> (Noah–LSM)     |
| Reference              | Ferrier et al.<br>(1995)  | Zhang et al.<br>(2011) | Janjic<br>(1994)                    | Iacono et al.<br>(2008)    | Tewari et al.<br>(2004) |

**Table 3.** Overview of time and location of maximum intensity (defined by the maximum of the Laplacian of mslp) of the TOP 30 MPI-ESM-P cyclones for PI and LGM conditions inside the box (Figure 1).

|    | PI      |      |        |       |        | LGM     |      |        |       |        |
|----|---------|------|--------|-------|--------|---------|------|--------|-------|--------|
|    | Date    | Time | Lapl P | °Lat  | °Lon   | Date    | Time | Lapl P | °Lat  | °Lon   |
| 1  | 2993010 | 18   | 3.162  | 51.54 | 342.98 | 1936021 | 00   | 3.535  | 52.33 | 338.93 |
| 2  | 2996010 | 12   | 3.158  | 51.96 | 343.35 | 1931101 | 18   | 3.430  | 47.35 | 335.87 |
| 3  | 2990112 | 18   | 2.858  | 44.31 | 340.09 | 1936112 | 00   | 3.220  | 46.53 | 341.67 |
| 4  | 2994110 | 18   | 2.811  | 41.67 | 339.00 | 1942102 | 06   | 3.202  | 52.34 | 345.53 |
| 5  | 2983031 | 06   | 2.786  | 45.87 | 335.95 | 1922011 | 06   | 3.067  | 46.62 | 337.56 |
| 6  | 2998013 | 00   | 2.734  | 49.97 | 336.31 | 1940022 | 12   | 2.965  | 50.20 | 348.23 |
| 7  | 2994111 | 06   | 2.628  | 49.90 | 343.87 | 1941111 | 06   | 2.962  | 49.70 | 343.95 |
| 8  | 2980011 | 18   | 2.615  | 47.33 | 347.16 | 1932111 | 00   | 2.917  | 52.11 | 346.19 |
| 9  | 2998022 | 18   | 2.572  | 49.45 | 335.94 | 1927112 | 06   | 2.911  | 43.70 | 337.33 |
| 10 | 2999102 | 12   | 2.551  | 50.82 | 345.56 | 1921122 | 06   | 2.894  | 45.19 | 345.36 |
| 11 | 2983123 | 06   | 2.541  | 41.97 | 336.09 | 1925111 | 18   | 2.850  | 46.88 | 348.18 |
| 12 | 2985112 | 12   | 2.528  | 48.60 | 349.10 | 1944012 | 00   | 2.823  | 43.52 | 335.73 |
| 13 | 2999020 | 18   | 2.512  | 43.76 | 344.89 | 1940032 | 18   | 2.812  | 49.81 | 335.18 |
| 14 | 2994020 | 12   | 2.511  | 46.31 | 345.74 | 1942011 | 00   | 2.746  | 52.13 | 337.36 |
| 15 | 2989122 | 00   | 2.493  | 51.81 | 342.91 | 1937102 | 00   | 2.728  | 45.43 | 348.59 |
| 16 | 2979022 | 00   | 2.491  | 50.35 | 344.83 | 1923032 | 18   | 2.725  | 50.70 | 349.34 |
| 17 | 3003120 | 06   | 2.489  | 42.45 | 344.77 | 1940110 | 18   | 2.688  | 51.82 | 346.50 |
| 18 | 3001010 | 18   | 2.473  | 48.50 | 339.35 | 1922010 | 06   | 2.679  | 42.31 | 342.38 |
| 19 | 2985011 | 18   | 2.471  | 43.52 | 338.38 | 1923020 | 12   | 2.678  | 48.73 | 342.70 |
| 20 | 2987010 | 12   | 2.466  | 47.53 | 345.43 | 1935010 | 18   | 2.663  | 51.29 | 339.74 |
| 21 | 2996112 | 00   | 2.457  | 46.23 | 337.72 | 1935121 | 00   | 2.635  | 52.12 | 342.00 |
| 22 | 3000122 | 06   | 2.299  | 47.43 | 345.84 | 1924022 | 00   | 2.613  | 50.39 | 344.81 |
| 23 | 2990022 | 18   | 2.298  | 51.33 | 348.96 | 1933110 | 06   | 2.611  | 51.09 | 341.01 |
| 24 | 2981121 | 06   | 2.272  | 47.65 | 345.85 | 1938100 | 12   | 2.590  | 51.91 | 336.29 |
| 25 | 2991011 | 00   | 2.263  | 49.51 | 338.82 | 1943021 | 06   | 2.584  | 48.11 | 348.10 |
| 26 | 2979112 | 12   | 2.252  | 45.25 | 349.74 | 1932021 | 06   | 2.507  | 49.92 | 345.95 |
| 27 | 3004011 | 06   | 2.246  | 44.70 | 340.05 | 1927011 | 06   | 2.497  | 47.66 | 341.06 |
| 28 | 2997021 | 18   | 2.200  | 48.06 | 343.77 | 1937120 | 00   | 2.481  | 43.06 | 336.95 |
| 29 | 3000032 | 00   | 2.167  | 50.88 | 341.08 | 1923020 | 00   | 2.478  | 50.41 | 347.84 |
| 30 | 3003103 | 18   | 2.147  | 46.78 | 347.93 | 1923022 | 12   | 2.448  | 42.46 | 345.65 |
|    | Mean    |      | 2.52   | 47.51 | 342.72 |         |      | 2.80   | 48.53 | 342.53 |
|    | Median  |      | 2.49   | 47.59 | 343.56 |         |      | 2.73   | 49.76 | 343.54 |

Figures

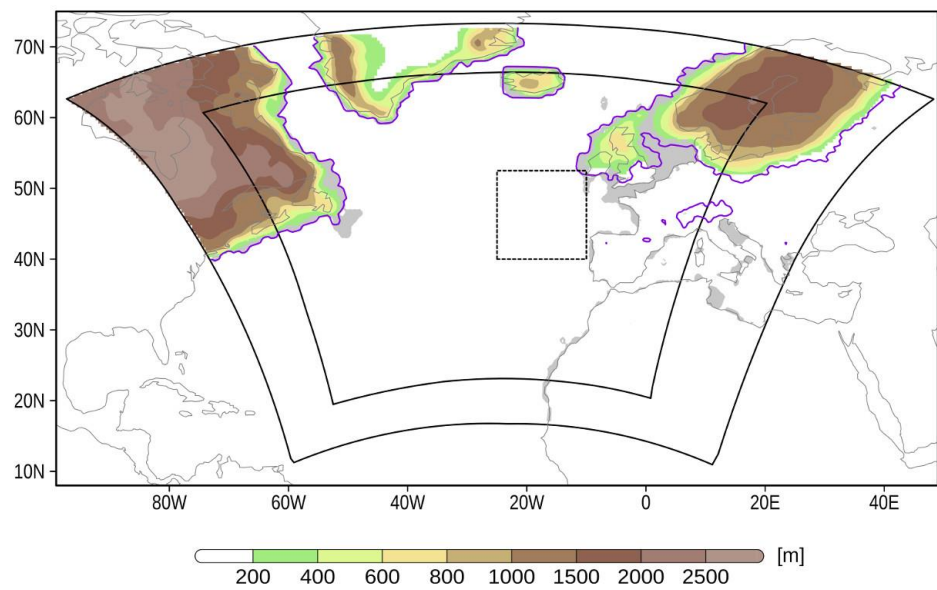


**Figure 1.** WRF model domains (outer solid box: 50 km grid spacing; inner solid box: 12.5 km grid spacing), ice sheet heights [m] (coloured) and **extents** (purple line), land sea mask (additional land areas grey) as obtained from PMIP3; target area for cyclone detection marked by dotted box.

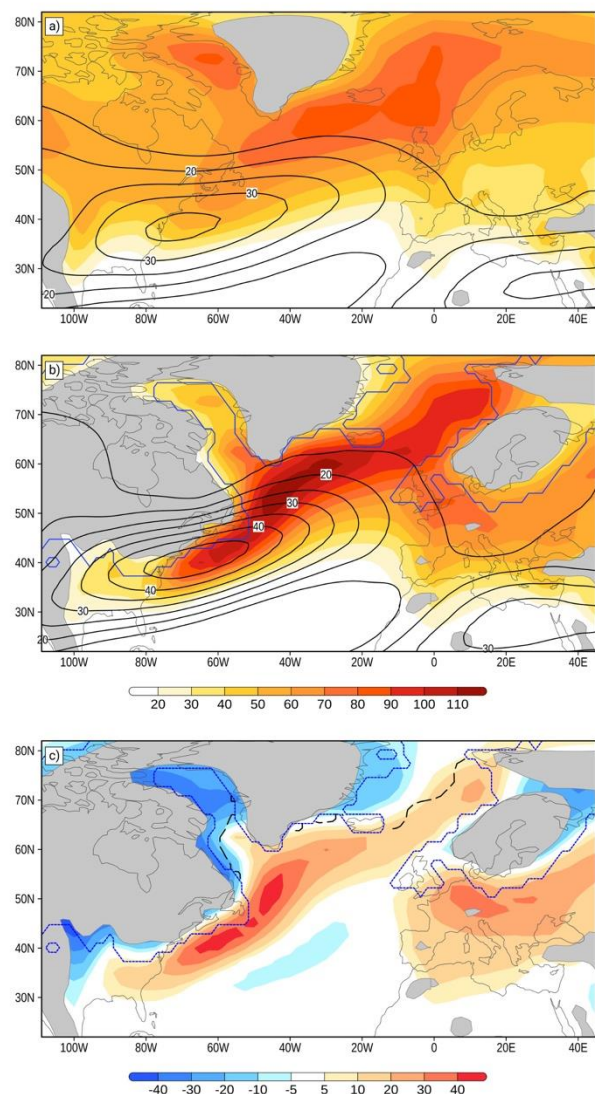


**Figure 2.** Cyclone track density [cyclone days per extended winter per (deg.lat.)<sup>2</sup>] (coloured) and 300 hPa wind speed [m s<sup>-1</sup>] (contours) based on MPI-ESM-P data for (a) PI, (b) LGM and (c) difference between LGM and PI. Areas with topography higher 1000 m shaded grey, ice sheet margins (b and c) denoted by thin stippled line, long dashed black line in (c) denotes margin of 40% annual sea ice cover.

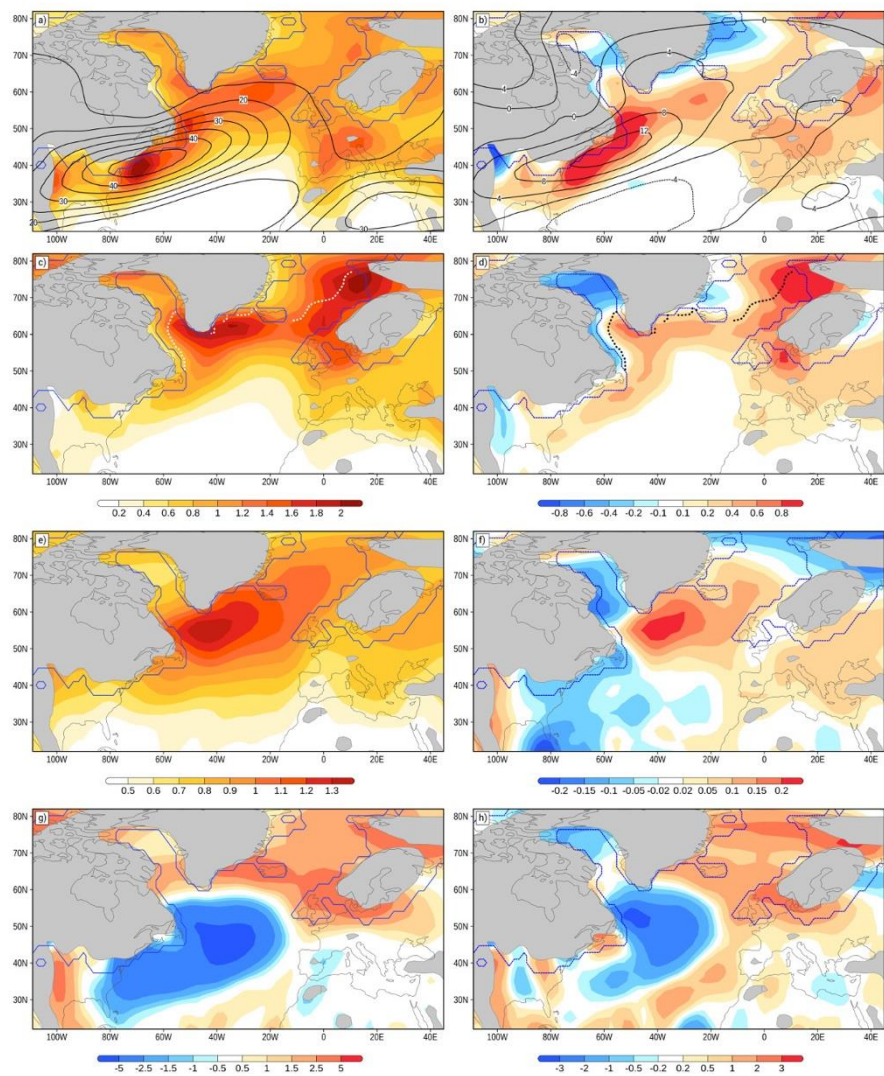


**Figure 3.** Statistical measures obtained from cyclone tracking algorithm for LGM cyclones (left column) and difference to PI cyclones (right column) for (a), (b) cyclogenesis [events per extended winter per (deg.lat.)<sup>2</sup>] (coloured) and wind speed at 300hPa [m s<sup>-1</sup>] (contours), (c),(d) cyclolysis [events per extended winter per (deg.lat.)<sup>2</sup>]; (e), (f) mean  $\Delta$  MSLP [Laplacian of pressure per extended winter per (deg.lat.)<sup>2</sup>] and (g), (h) deepening rates [hPa h<sup>-1</sup>]. Areas with topography higher 1000 m shaded grey, ice sheet extents marked by the blue line. Sea ice margin (>40% annual cover) in (c) and (d) indicated by bold dashed lines.

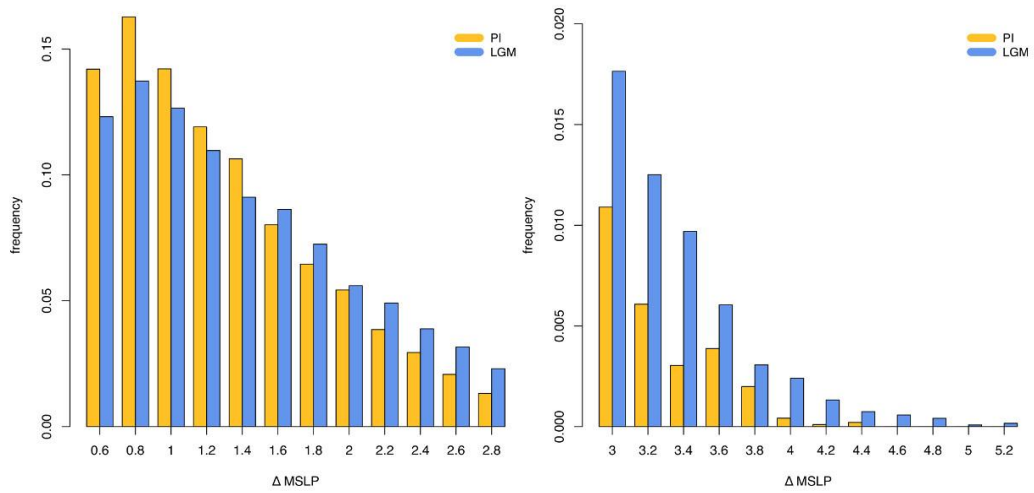


**Figure 4.** Histogram of cyclone intensity (Laplacian ( $\Delta$ ) MSLP) over the North Atlantic ( $70^\circ\text{W} - 0^\circ$  and  $35^\circ\text{N} - 70^\circ\text{N}$ ). For intense cyclones ( $\Delta P \geq 3$ ), the y-axis is **adjusted (right panel)**.



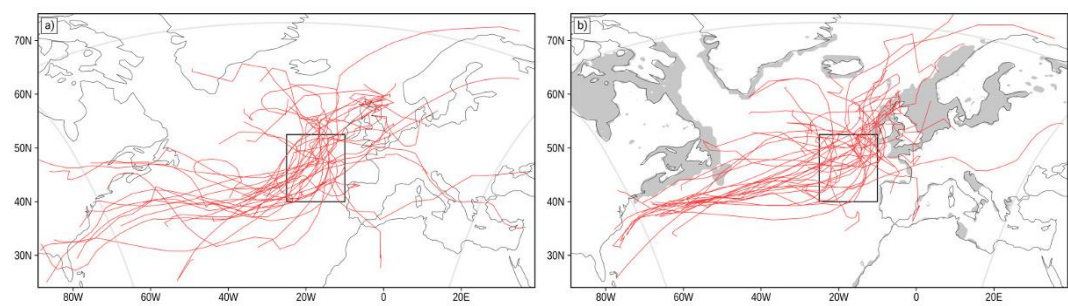
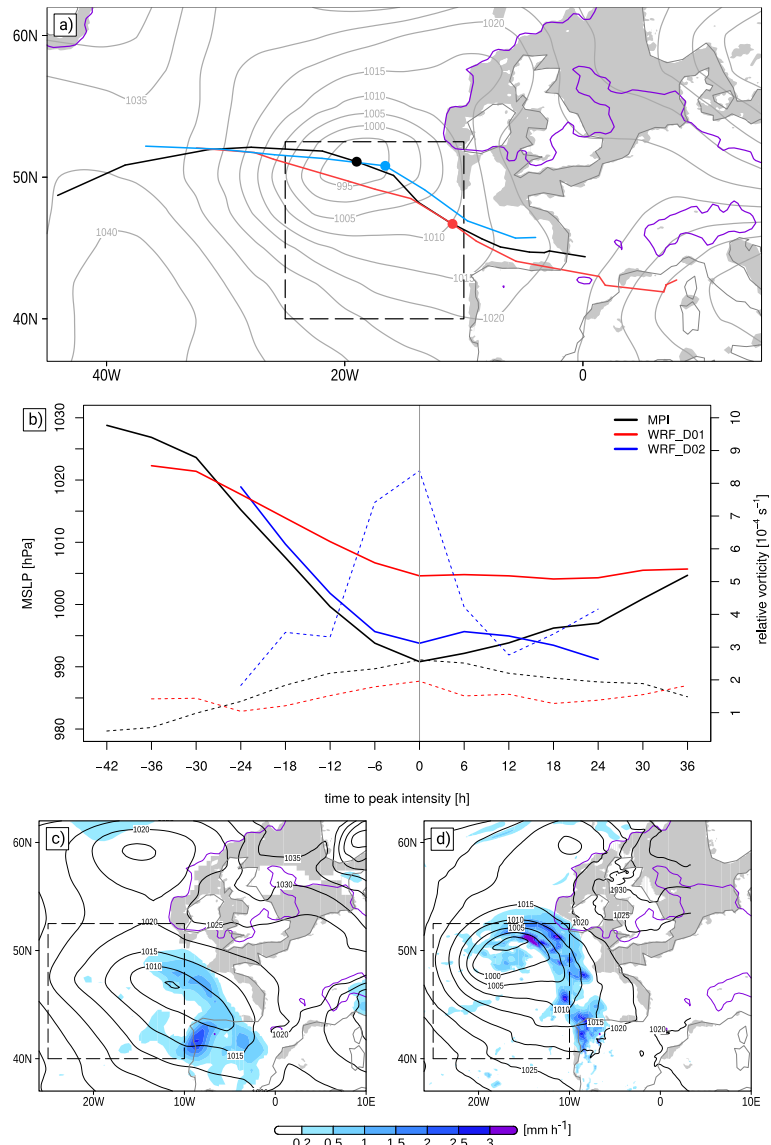
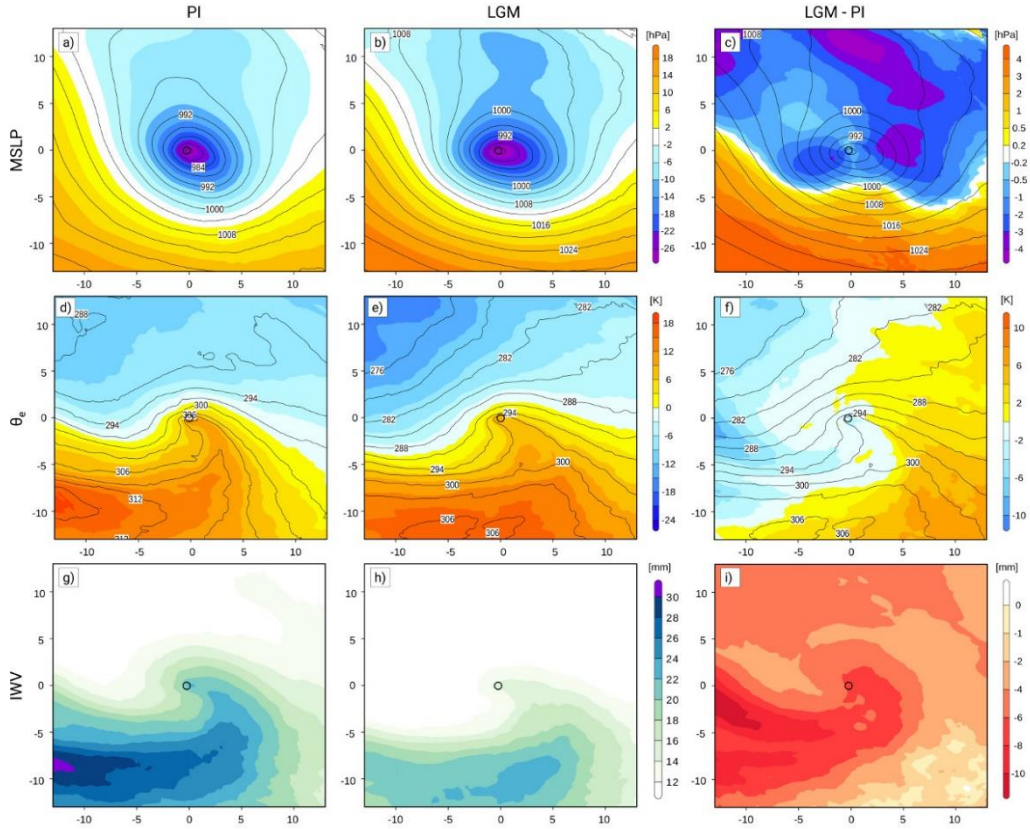


Figure 5. Cyclone tracks of TOP 30 (a) PI and (b) LGM cyclones (MPI-ESM). Black box is region where cyclones need to have maximum intensity to be considered in the composite analysis.



**Figure 6.** Comparison of (a) cyclone tracks for MPI-ESM (black), WRF 50km (red) and WRF 12.5 km (blue) (coloured dots mark the location of peak intensity, black dotted box shows target area) and MSLP [hPa] for MPI-ESM at peak intensity, (b) timeseries of cyclone core pressure and relative vorticity for MPI-ESM, WRF 50km and WRF 12.5 km for LGM cyclone #24. Simulated precipitation rate [ $\text{mm h}^{-1}$ ] (shaded) and MSLP [hPa] (lines) at peak intensity for (c) WRF 50km and (d) WRF 12.5km.



**Figure 7.** Composites of (a - c) mean sea level pressure, (d - f) ThetaE, and (g - i) vertical integrated water vapour (IWV) for PI, LGM and difference LGM – PI at peak intensity as defined by the maximum of the Laplacian of MSLP. (a, b) absolute MSLP values (lines, [hPa]), anomalies [hPa] from mean over displayed area (coloured); (c) absolute MSLP values (lines, [hPa]) from LGM, differences of the anomalies between LGM – PI in colours; (d, e) absolute ThetaE values (lines, [K]) and anomalies [K] from mean over displayed area (coloured); (f) absolute ThetaE values (lines, [K]) from LGM, differences of the anomalies between LGM – PI in colours; (g, h) absolute IWV values [mm], (i) difference [mm] LGM – PI.

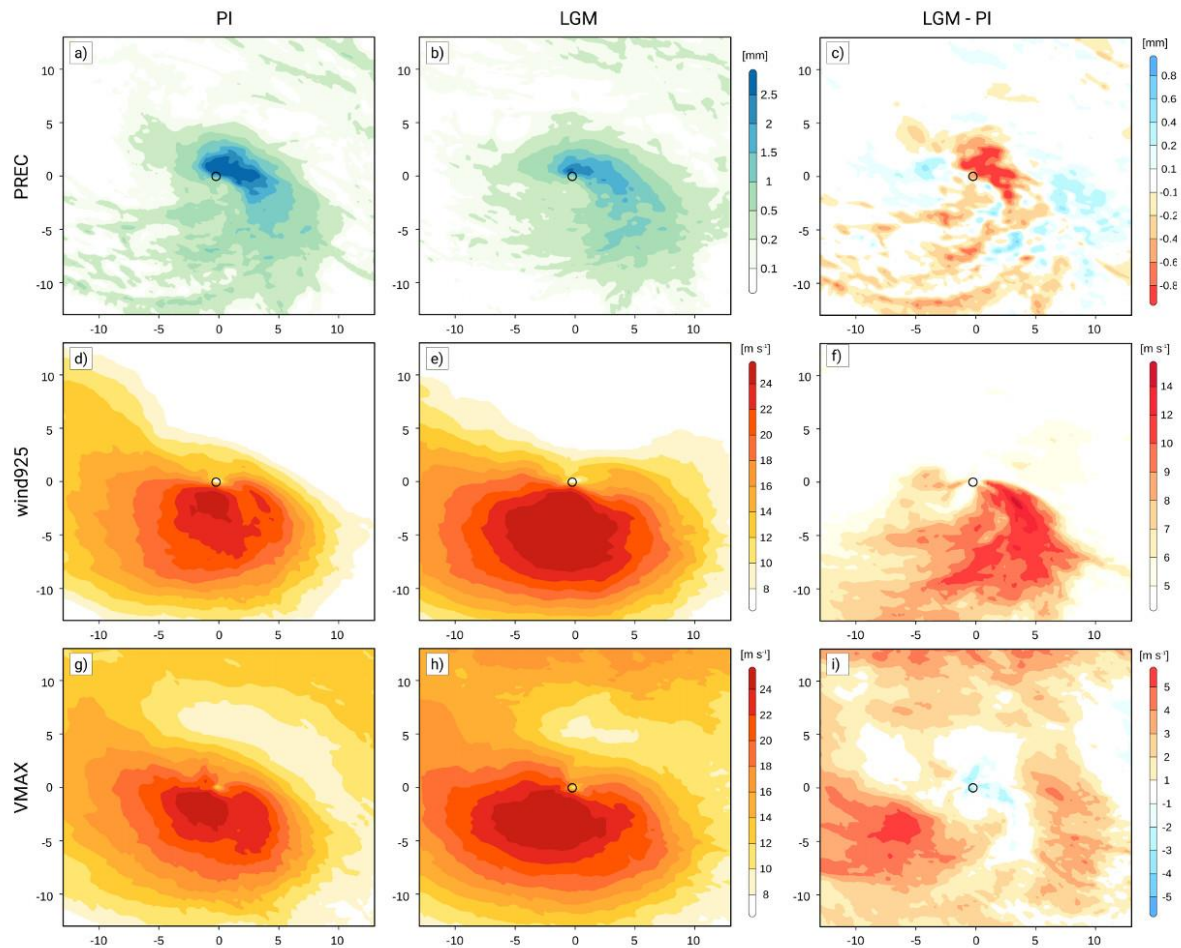


**Figure 8.** As Figure 7 but for hourly precipitation [mm] (a) PI, (b) LGM, (c) LGM – PI, (d - f) wind speed in 925 hPa [ $\text{m s}^{-1}$ ] and (g - i) maximum near surface wind gust [ $\text{m s}^{-1}$ ] at peak intensity.

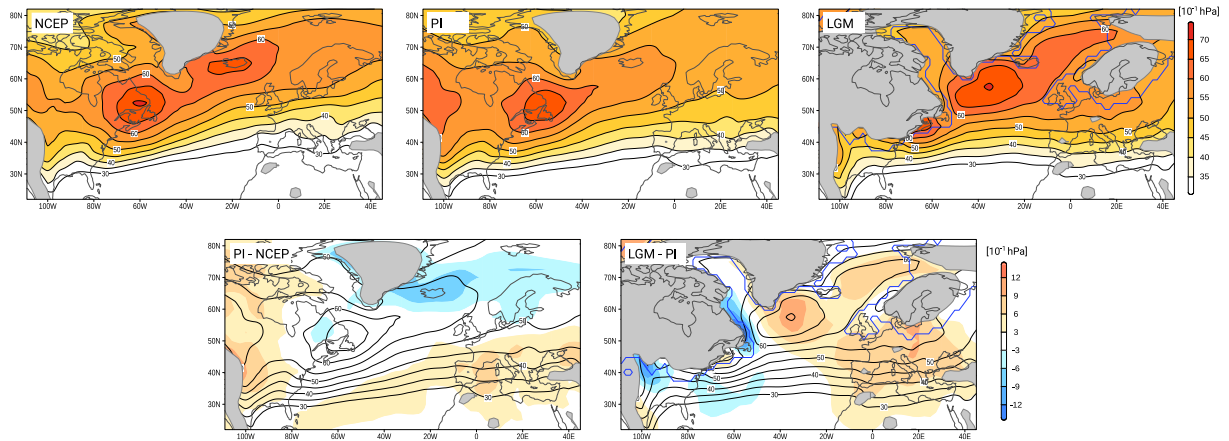


Fig. S1: Top: storm tracks (2–6 days band passed filter of daily MSLP data [ $1/10$  hPa]) for the NCEP Reanalysis data and the MPI-ESM-P simulations for PI and LGM. Bottom: differences (shaded) between PI (lines) and NCEP and between LGM (lines) and PI. Areas with topography higher 1000 m shaded grey, LGM ice sheet extent marked by the blue line.

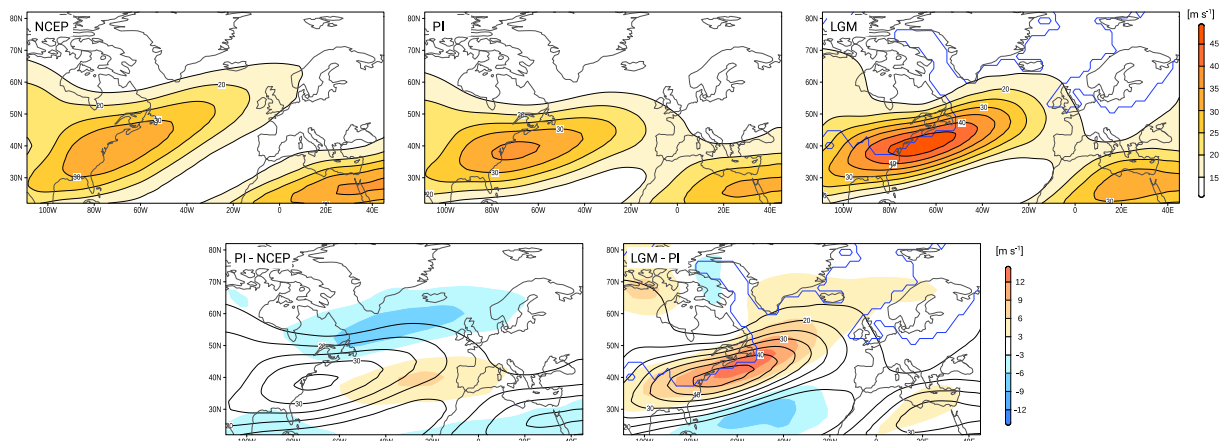
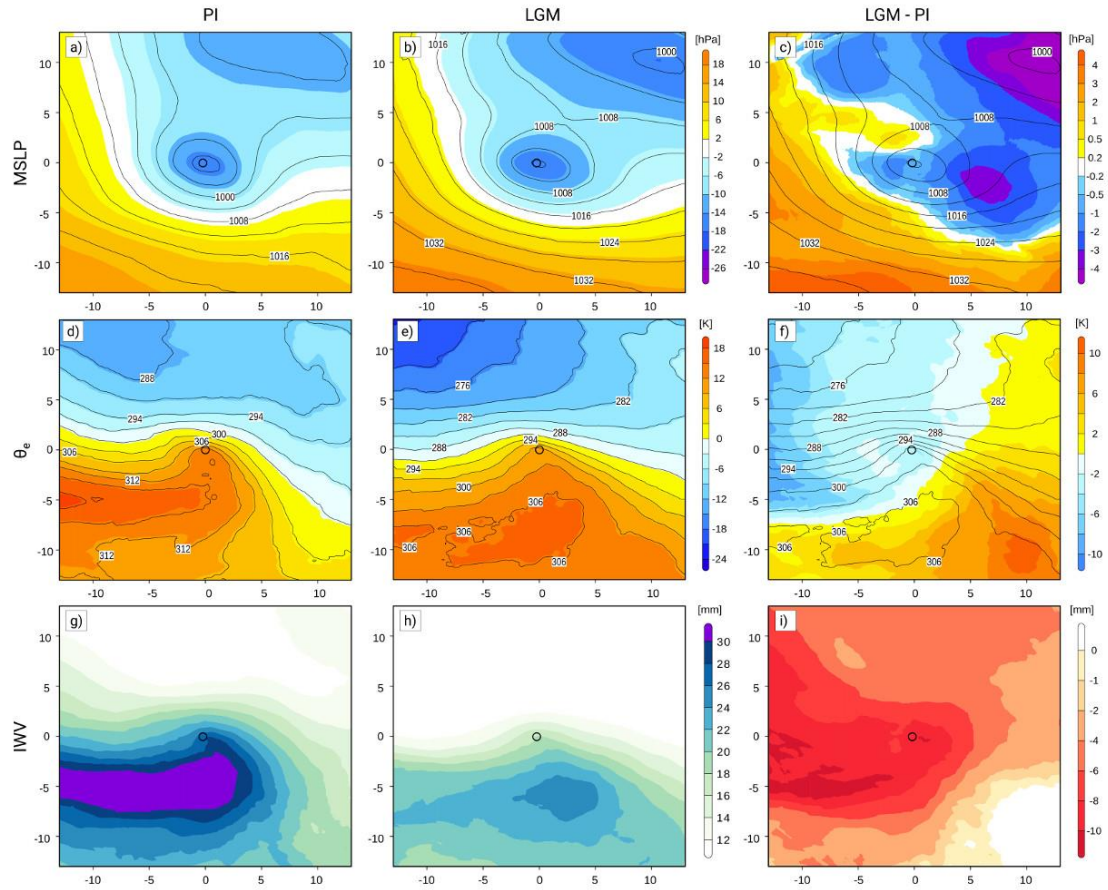
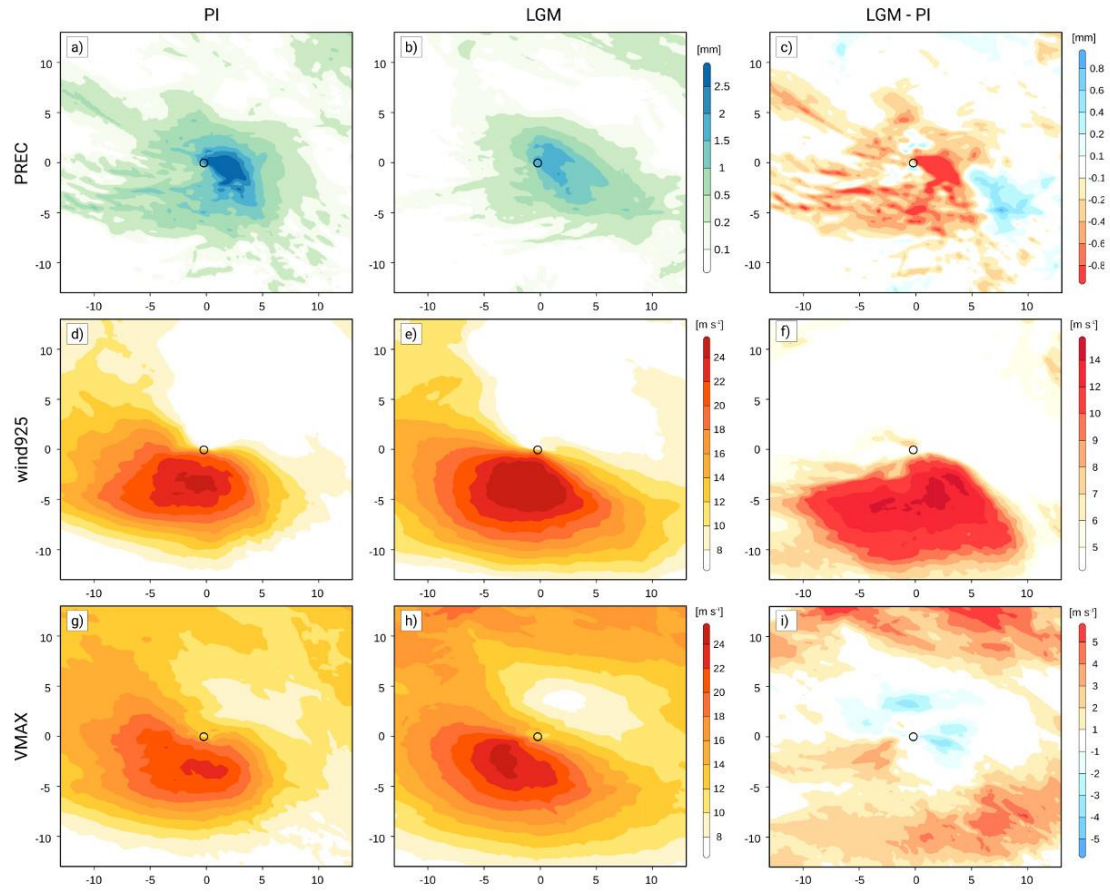


Fig. S2: Top: Upper level jet stream (wind speed at 300 hPa [ $\text{m/s}$ ]) for the NCEP Reanalysis data and the MPI-ESM-P simulations for PI and LGM. Bottom: differences (shaded) between PI (lines) and NCEP and between LGM (lines) and PI. LGM ice sheet extent marked by the blue line.





**Figure S3.** Composites of (a - c) mean sea level pressure, (d - f) ThetaE, and (g - i) vertical integrated water vapour (IWV) for PI, LGM and difference LGM – PI 12 hours before peak intensity as defined by the maximum of the Laplacian of MSLP. (a, b) absolute MSLP values (lines, [hPa]), anomalies [hPa] from mean over displayed area (coloured); (c) absolute MSLP values (lines, [hPa]) from LGM, differences of the anomalies between LGM – PI in colours; (d, e) absolute ThetaE values (lines, [K]) and anomalies [K] from mean over displayed area (coloured); (f) absolute ThetaE values (lines, [K]) from LGM, differences of the anomalies between LGM – PI in colours; (g, h) absolute IWV values [mm], (i) difference [mm] LGM – PI.



**Figure S4.** As Figure S3 but for hourly precipitation [mm] (a) PI, (b) LGM, (c) LGM – PI, (d - f) wind speed in 925 hPa [ $\text{m s}^{-1}$ ] and (g - i) maximum near surface wind gust [ $\text{m s}^{-1}$ ] 12 hours before peak intensity.



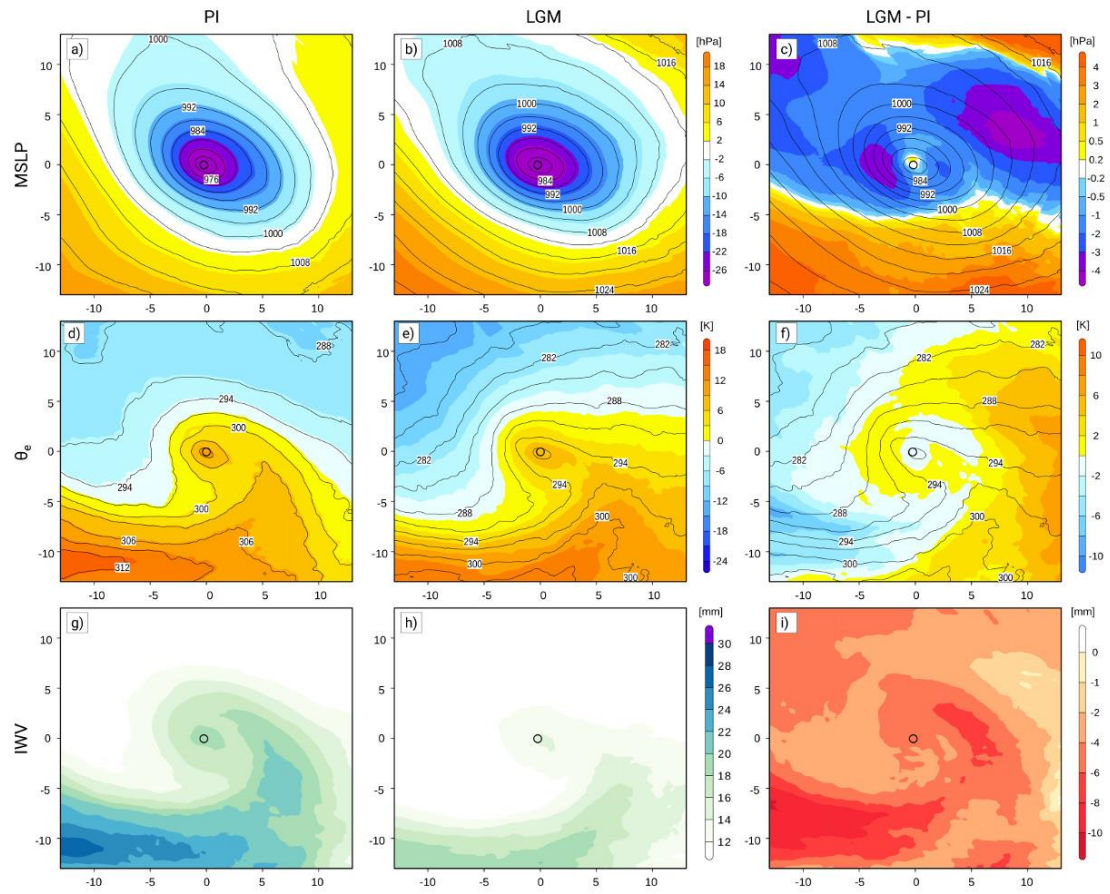


**Figure S5.** As Figure S3 but 12 hours after peak intensity.

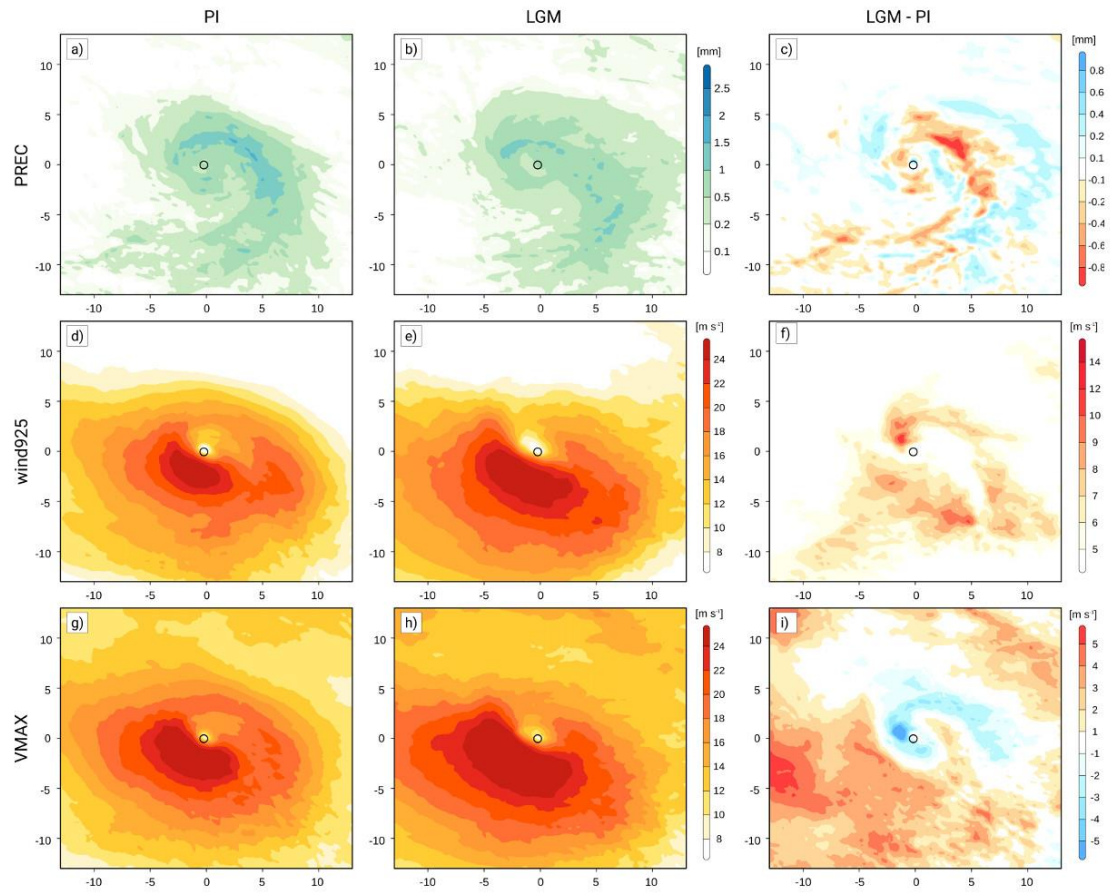


**Figure S6.** As Figure S4 but for 12 hours after peak intensity.

Table S1: Summary of wind speed at 925 hPa, maximum near surface wind gust and total precipitation of the TOP 30 PI and LGM ensemble with 12.5 km resolution for 12 hours before / after and at peak intensity. Field mean and maximum corresponds to area depicted in Fig. S4, Fig. S6 and Fig. 8.

|     | wind925<br>(mean) [m/s] |       | wind925<br>(max) [m/s] |       | VMAX<br>(mean) [m/s] |       | VMAX<br>(max) [m/s] |       | PREC (mean)<br>[mm/h] |      | PREC (max)<br>[mm/h] |      |
|-----|-------------------------|-------|------------------------|-------|----------------------|-------|---------------------|-------|-----------------------|------|----------------------|------|
|     | PI                      | LGM   | PI                     | LGM   | PI                   | LGM   | PI                  | LGM   | PI                    | LGM  | PI                   | LGM  |
| -12 | 9.56                    | 11.37 | 24.71                  | 27.23 | 12.46                | 14.10 | 23.04               | 25.24 | 0.29                  | 0.20 | 3.45                 | 2.05 |
| 0   | 10.67                   | 12.25 | 25.96                  | 27.95 | 13.47                | 15.49 | 26.84               | 26.98 | 0.28                  | 0.24 | 3.56                 | 2.70 |
| 12  | 11.69                   | 12.91 | 26.68                  | 28.82 | 14.50                | 16.09 | 28.66               | 30.31 | 0.24                  | 0.24 | 1.66                 | 1.27 |